Magnetic Resonance Materials in Physics, Biology and Medicine (2022) 35:503–521
https://doi.org/10.1007/s10334-022-01006-6

REVIEW

The role of MRI in prostate cancer: current and future directions

Maria Clara Fernandes[1] · Onur Yildirim[1] · Sungmin Woo[1] · Hebert Alberto Vargas[1] · Hedvig Hricak[1]

Received: 16 July 2021 / Revised: 16 January 2022 / Accepted: 3 March 2022 / Published online: 16 March 2022

Abstract

There has been an increasing role of magnetic resonance imaging (MRI) in the management of prostate cancer. MRI already plays an essential role in the detection and staging, with the introduction of functional MRI sequences. Recent advancements in radiomics and artificial intelligence are being tested to potentially improve detection, assessment of aggressiveness, and provide usefulness as a prognostic marker. MRI can improve pretreatment risk stratification and therefore selection of and follow-up of patients for active surveillance. MRI can also assist in guiding targeted biopsy, treatment planning and follow-up after treatment to assess local recurrence. MRI has gained importance in the evaluation of metastatic disease with emerging technology including whole-body MRI and integrated positron emission tomography/MRI, allowing for not only better detection but also quantification. The main goal of this article is to review the most recent advances on MRI in prostate cancer and provide insights into its potential clinical roles from the radiologist's perspective. In each of the sections, specific roles of MRI tailored to each clinical setting are discussed along with its strengths and weakness including already established material related to MRI and the introduction of recent advancements on MRI.

Keywords Prostate cancer · MRI · Diffusion-weighted imaging · Dynamic contrast-enhanced MRI · Active surveillance · Metastasis · Staging · Biochemical recurrence

Abbreviations

ADC	Apparent diffusion coefficient
ADT	Androgren-deprivation therapy
AUC	Area under the receiver operating characteristic curve
BCR	Biochemical recurrence
BS	Bone scintigraphy
CADx	Computed-aided diagnosis
csPCa	Clinically significant prostate cancer
CT	Computed tomography
DCE	Dynamic contrast-enhanced
DL	Deep learning
DRE	Digital rectal exam
DWI	Diffusion-weighted imaging
EPE	Extraprostatic extension
GS	Gleason score
MET-RADS-P	METastasis reporting and data system for prostate cancer
mpMRI	Multiparametric magnetic resonance imaging
MRI	Magnetic resonance imaging
MRI-Tb	Magnetic resonance imaging-targeted biopsy
MRS	Magnetic resonance spectroscopy
NCCN	National comprehensive cancer network
NVB	Neurovascular bundle
PET	Positron emission tomography
PI-RADS	Prostate imaging reporting and data system
PI-RR	Prostate imaging for recurrence reporting
PSA	Prostate-specific antigen
PSMA	Prostate-specific membrane antigen
PRECISE	Prostate cancer radiological estimation of change in sequential evaluation
SVI	Seminal vesicle invasion
T1WI	T1-weighted image
T2WI	T2-weighted image
US	Ultrasound

Maria Clara Fernandes and Onur Yildirim contributed equally.

✉ Sungmin Woo
woos@mskcc.org

[1] Department of Radiology, Memorial Sloan Kettering Cancer Center, 1275 York Ave, New York, NY 10065, USA

Introduction

There has been an increasing role of magnetic resonance imaging (MRI) in the management of prostate cancer with advances in technology. These include the introduction of functional sequences (e.g., dynamic contrast-enhancement [DCE] MRI and diffusion-weighted imaging [DWI]), high-field magnets (e.g., 3-Tesla), whole-body MRI, and hybrid imaging (e.g., integrated positron emission tomography [PET]/MRI). MRI plays key roles in many steps of prostate cancer management, including detection and diagnosis, MRI-guided biopsy, staging, active surveillance, treatment planning, evaluation of biochemical recurrence, and assessment of metastatic disease. In the following sections, the role of MRI in each clinical setting is discussed along with its strengths and weaknesses. The scope of this article is to review not only already established material related to MRI but also introduce the recent advancements on MRI and provide insights into its potential clinical roles.

Detection and diagnosis of prostate cancer

Limitations of conventional modalities

Traditionally, abnormal digital rectal exam (DRE) results and elevated serum prostate-specific antigen (PSA) levels have often been used to diagnose prostate cancer. However, these approaches are neither sensitive nor specific. For example, 70–80% of patients with elevated PSA levels (>4 ng/mL) do not have prostate cancer [1]. Ultrasound (US) has a limited role in detecting prostate cancer as focal lesions are visible only in a small proportion of patients (11–35%). Among them, only a small proportion (17–57%) are subsequently revealed to be tumors. Therefore, the US is currently used to visualize the prostate (but not the prostate cancer itself, unless there is a sonographic correlate that matches the location of the focal lesion seen on MRI during cognitive fusion biopsy) during transrectal or transperineal US-guided biopsies. Computed tomography (CT), although some studies have demonstrated a potential role for detecting very high-grade tumors given its high specificity, is not an optimal imaging tool for diagnosing prostate cancer due to its lack of soft tissue detail and molecular information [2].

Role of MRI as a standard of care

When compared to the above methods, magnetic resonance imaging (MRI) has superior ability in detecting the index primary prostatic lesion. Especially with the advances in technology and the currently established multiparametric MRI (mpMRI) protocol (which is discussed in detail below) is now commonly used for detecting, staging, and planning treatment of prostate cancer. The PROMIS study on prostate magnetic resonance imaging (MRI) is a compelling example with mpMRI showing significantly higher sensitivity for identifying clinically significant cancer: 93% for MRI and 48% for transrectal US-guided biopsy. Recent research findings are already being used in medical practice [3].

Multiparametric MRI protocol and interpretation

MpMRI protocols for detecting/diagnosing prostate cancer consist of the following sequences, to increase sensitivity and specificity by combining anatomical sequences of T1-weighted images (T1WI) and multiplanar T2-weighted images (T2WI) with functional sequences of DWI and DCE-MRI. The anatomical detail of the prostate can be clearly depicted by MRI, with superior soft tissue resolution T1WI for prostate vs periprostatic fat) and zonal anatomy (T2WI imaging for differentiating peripheral, transition, and central zones). Recent guidelines such as the prostate imaging reporting and data system (PI-RADS), now with the most recent version 2.1, make the use of endorectal coils optional, provided that MRI parameters are optimized on scanners with 1.5- or 3-Tesla magnets with multichannel pelvic phased-array receiver coils [4]. MR spectroscopy (MRS) is no longer routinely recommended due to its technical challenges and difficulty in widespread usage across academic and community-based practices. In addition, there has been downgrading in the importance of DCE-MRI with a merely positive vs negative assessment recommended in the PI-RADS guidelines. Some further advocate the usage of biparametric MRI using only T2WI and DWI owing to the minimal added benefit of DCE-MRI in the pretreatment setting considering added time, cost, and potential contrast reactions [5]; whereas, others still support its usage for better diagnosis and characterization of focal lesions and are investigating ways to optimize the interpretation of DCE-MRI (e.g., optimal cut-off timing and shape to determine positivity) [6–8]. Nevertheless, acquisition with multi- or bi-parametric MRI and interpretation with a standardized scheme of PI-RADS has accelerated the widespread adoption of prostate MRI at many leading centers and community-based practices. A recent meta-analysis concluded that the PIRADS v2 has a good sensitivity of 0.89 (95% CI 0.84–0.92) and specificity of 0.73 (95% CI 0.46–0.78) for detecting prostate cancer [9]. Nevertheless, there is still a large degree of variation (even amongst centers with high expertise) as shown in a recent multicenter study: positive predictive value of PI-RADS score of ≥3 for detecting clinically significant prostate cancer (csPC) ranging from 27% to 48% in 26 centers [10].

MRI-targeted biopsy

The ability of MRI to improve prostate cancer detection over the past few decades has allowed MRI to play a greater role in diagnosis rather than just staging. This additionally led to a "paradigm shift" from TRUS-guided biopsy to MRI-targeted- or guided-biopsy (MRI-Tb). The rationale for MRI being used for targeted biopsy is its high negative predictive value (89%) for the diagnosis of csPCa [11]. In addition, randomized controlled trials including the PRECISION trial have shown that MRI-stratified pathways, either by using MRI-Tb alone or in conjunction with systematic US-guided biopsies, detect more csPC with a relative diagnosis rate of 1.45 compared with transrectal US-guided biopsy [12, 13]. The PROMIS trial suggests that approximately a quarter of men could avoid prostate biopsy if mpMRI were used as a triage test owing to its high negative predictive value (89% for mpMRI and 74% for TRUS) [3]. Similar results have been shown recently in a population-based noninferiority trial of prostate cancer screening where in 1532 men with PSA levels of 3 ng/ml or higher (among 12,750 enrolled men), MRI-Tb with systematic biopsies performed only in those with positive prostate MRI resulted in similar detection of csPC and decreased detection of insignificant prostate cancer compared with undergoing a systematic biopsy, indicating that this MRI-directed pathway may be able to have a large impact on management [14]. Nevertheless, a non-negligible proportion of csPCa are missed on MRI—for instance, 16% (26/162) in a study correlating MRI and whole-mount radical prostatectomy specimens [15]—and, therefore, it should be emphasized that a "safety net" consisting of a combination of clinical, laboratory, and imaging assessments as per local clinical practice needs to be in place if a patient opts out of biopsy because of a negative MRI result [16].

Radiomics, computer-aided diagnosis, and artificial intelligence

Radiomics models have been extensively evaluated as a means to provide a non-invasive tool for detecting and determining the aggressiveness of prostate cancer. It obtains properties that are undetectable to the human eye (e.g., textures or features) on various sequences (e.g., T2WI, DWI, DCE-MRI, and MRS) that are potentially thought to be related to the microstructure and microenvironment, which can be used as feedback for traditional classifier models [17, 18]. Although early results were promising, they have yet to be incorporated into routine clinical practice due to many reasons. For example, different models yield varying degrees of accuracy for different tasks, generalizability is lacking as most models are specific to and are overfitted to the population that they were developed in [19]. Therefore, many are still regarded as "proof-of-concept", given the small number of patients and single-center retrospective nature. For instance, one prostate computed-aided diagnosis (CADx) device reported an extremely high area under the receiver operating characteristic curve (AUC) of 0.96 for detecting prostate cancer [20]. On the contrary, several other prostate CADx systems lower AUCs ranging from 0.80 to 0.89 [21]. Most of these systems require manual selection of ROIs to produce lesion candidates, and in turn render the results specific to the system and the operator. Nevertheless, the increasing interest in AI techniques and their applications in medicine has influenced the development of computer-aided diagnosis (CADx) systems for detecting, grading, and introducing new classifications of prostate cancer [22–26]. With further internal and external validation (potentially in multicentral and prospective settings), it is expected that in the near future such techniques will make its way into our daily clinical practice, increasing our diagnostic performance, confidence, and efficiency.

A few promising examples of radiomic models that have been used for initial assessment of prostate cancer include: identifying lesions [27, 28], distinguishing low- from higher-grade prostate cancer [29], predicting Gleason score (GS) [17, 18, 30], and planning radiotherapy [31–33]. Furthermore, radiomics can also be used to better classify PI-RADS v2.1 categories [34]. In addition to these, radiomic models have recently also been investigated for their association with genetic traits (e.g., radiogenomics), further allowing the possibility of identifying the inherent biological aggressiveness of prostate cancer [35, 36]. For example, MRI was able to direct biopsies to the most suspicious regions of the prostate, increasing the efficiency and sensitivity of sampling for key molecular markers such as p53, which was associated with shorter recurrence-free survival in patients after radical prostatectomy. [37].

There have been remarkable advances in "deep learning" (DL) in the field of medical imaging analysis, and early promising results have been published over the past few years. Schelb et al. [38] developed a U-net-based DL algorithm for detecting suspicious lesions on prostate MRI in men suspected of having clinically significant cancer, and reported high sensitivities of 92–96%. Vos et al. [39] showed that DL-CADx method may be able to assist radiologists in selecting locations of prostate cancer and could help direct biopsy to the most aggressive area. Winkel et al. [40] found that DL-based CADx not only improved the accuracy of finding suspicious lesions but also was able to reduce inter-reader variability. In all the above studies, higher sensitivity of the DL-based algorithm was associated with higher false-positive rates, which is an obstacle that needs to be overcome before widespread implementation into clinical practice. Furthermore, future studies need to demonstrate an agreement between the algorithm and the human reader

to be at least comparable to human interobserver metrics and develop user-friendly interface and workflow integration schemes [41].

Another area that future studies could focus on is the importance of the zonal location of prostate cancer. Transition zone and peripheral zone cancers often demonstrate different quantitative features on MRI and, therefore, computer-extracted parameters from tumors in the peripheral zone may be inapplicable for usage in the transition zone. Most of the current research up to now focused on entire prostate cancer instead of analyzing each zone separately. In addition, future research on radiomics and CADx for prostate cancer diagnosis needs to focus on comprehensively using the entirety of mpMRI data, as opposed to earlier studies assessing single sequences (e.g., T2WI). T2WI plus DWI and/or DCE-MRI are optimal and popular options, given their potential to provide both anatomical and functional information [42–44]. For example, Chan et al. [45] merged T2W, DWI, proton density, and T2 maps to predict the anatomical and textural features of the peripheral zone. Based on multichannel statistical classifiers, they created a summary statistical map of the peripheral zone that took into account the textural and anatomical features of PCa areas derived from T2W, DWI, proton density maps, and T2 maps. DCE-MRI and pharmacokinetic parameter maps were added to a CADx system by Langer et al. [46] for the detection of prostate cancer at the peripheral zone. A two-stage CADx system was developed by Vos et al. [39] using a blob detection approach in combination with segmentation and classification of the candidates utilizing statistical region features. Using a combination of segmentation, voxel classification, candidate extraction and classification, Litjens et al. [47] recently introduced a fully automated computer-aided detection system. In these studies, it was shown that it is feasible to distinguish benign tissues from malignant ones successfully [46, 47].

Integrated PET/MRI

A recent development in PET/MRI scanner technology has introduced the possibility of combining metabolic/receptor information from PET and anatomical and functional imaging from MRI in a multimodal manner. While most of the studies on PET/MRI have been on restaging for prostate cancer after treatment, diagnosis of the dominant lesion and characterization using PET/MRI has been an area of increasing interest in recent years, especially with the development of prostate-specific membrane antigen (PSMA) radioligands. Studies have shown that using PSMA PET/MRI can improve the diagnosis of csPC compared with mpMRI alone. For example, Ferraro et al. [48], shows that patient-based sensitivity and specificity were 96% and 81%, respectively. Additional studies by Park et al. [49], and Hicks et al. [50] showed that 68 Ga-PSMA-11 PET/MRI had a higher PPV than mpMRI for bilateral tumors (70% vs. 18%, respectively). Nevertheless, to determine whether PSMA PET/MRI should be used for the initial diagnosis and guiding biopsy as opposed to the current standard of mpMRI in terms of diagnostic accuracy and costs, further research is required.

Primary tumor staging

Upon diagnosis of a prostate lesion, the next step is staging. MRI is increasingly being used for staging prostate cancer, especially to improve the identification of extraprostatic extension (EPE) and seminal vesicle invasion (SVI). It is vital to accurately stage locally invasive prostate cancer through mpMRI. The presence of extraprostatic extension manifests as T2WI as broad capsular contact, capsular bulging and irregularity, rectoprostatic angle obliteration, and neurovascular bundles asymmetry [51] (Fig. 1). Features of the seminal vesicle invasion include homogeneous T2 signal hypointensity of the seminal vesicle, tumor location at the prostate base, loss of standard seminal vesicle tubular geometry, and related diffusion restriction [52] (Fig. 2). As reported by de Rooij et al. [53], mpMRI has a moderately high sensitivity, but very high specificity (0.61 and 0.88, respectively) when it comes to determining EPE and SVI. Most of the evidence has been based on qualitative analysis, including a Likert scale for the probability of EPE, and it has been suggested that accuracy is affected by the level of expertise [54, 55]. In addition to the detection of EPE and SVI (T3 stage), MRI is also useful for identifying invasion to adjacent structures such as external sphincter, rectum, bladder, levator muscles, and/or pelvic wall (T4 stage) [56] (Fig. 2).

Recent efforts have concentrated on identifying quantitative and more reproducible methods for assessing EPE and SVI. Tumor size (>12–14 mm) and volume assessed by not only MRI but also the US have been found to be independent predictors of EPE [57, 58]. Increasing capsular contact length has also been shown to be associated with a higher risk of EPE. Optimal threshold values for predicting EPE were >14, >13, >12, and >14 mm using the capsular contact length on T2WI, apparent diffusion coefficient (ADC) maps, DCE-MRI, and the maximum values among them, respectively [57]. In several studies, tumor ADC values have been shown to estimate EPE more accurately than T2WI alone [59]. Quantitative parameters from DCE-MRI, such as plasma flow and mean transit time have also shown promising results. Additionally, using standardized interpretation schemes such as the PI-RADS v2.1 has been shown to increase diagnostic accuracy and improve inter-reader agreement [60]. More recently, integrated PSMA PET/MRI has been gaining interest as a multimodal approach to improve

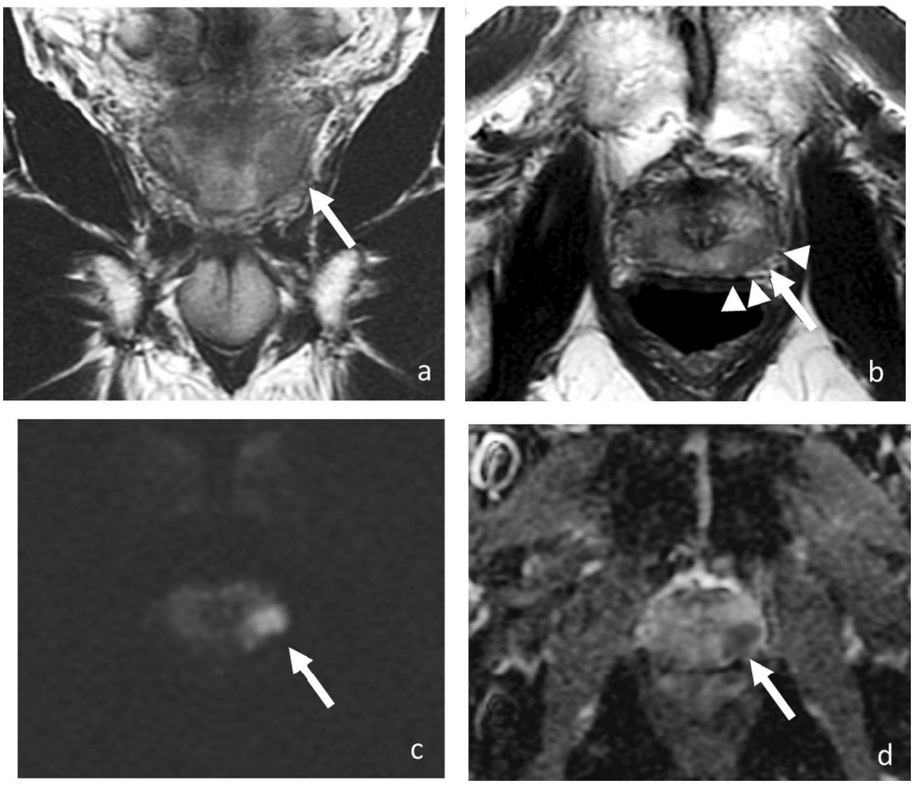

Fig. 1 Coronal (**a**) and axial T2-weighted images (**b**), DWI (**c**), and ADC (**d**). MRI of 68-year-old man with PSA of 7.73 ng/ml shows a 1.7-cm T2 hypointense lesion with marked restricted diffusion (arrow) in the left mid-gland peripheral zone with broad capsular contact and bulging (arrowheads). At radical prostatectomy, pathology revealed Gleason 4 + 3 prostate cancer with extraprostatic extension

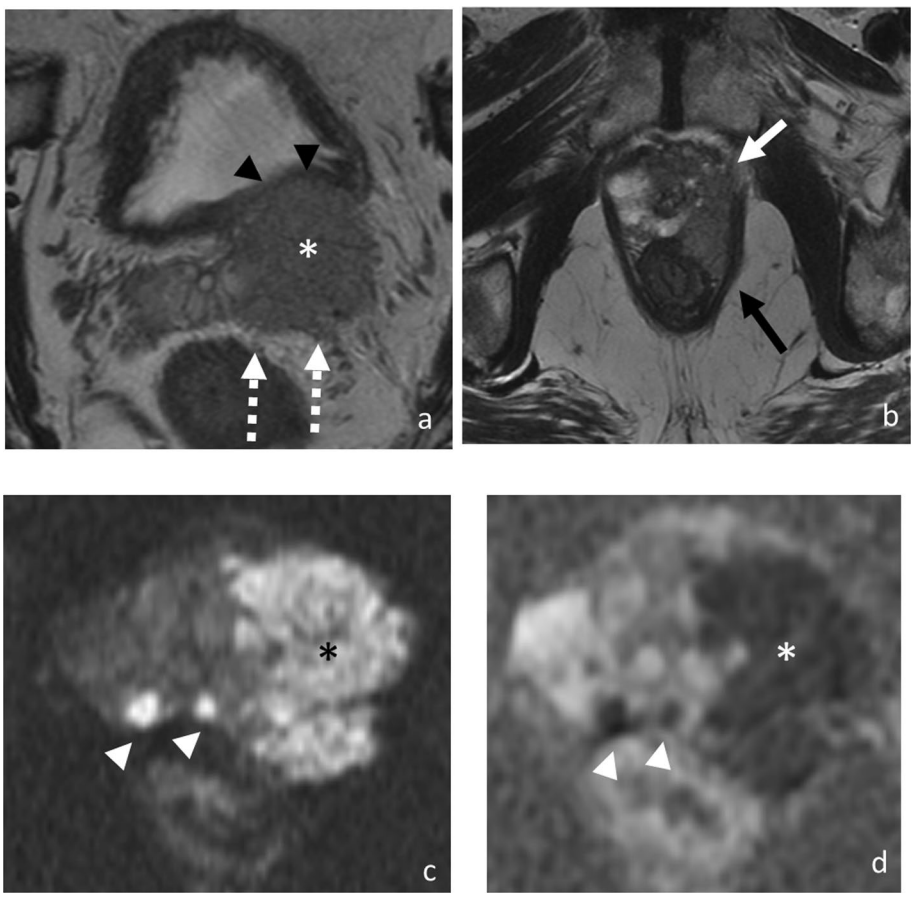

Fig. 2 Axial T2-weighted images (**a**,**b**), DWI (**c**), and ADC (**d**). MRI of 77-year-old man with a PSA of 123.97 ng/ml shows bilateral multifocal peripheral zone lesions with a 4.9 cm dominant lesion (asterisk) in the left prostate demonstrating multifocal extraprostatic extension, left seminal vesicle invasion (broken arrows), and invasion of the posterior bladder wall (black arrowheads), left anterolateral rectal wall (black arrow) and left levator ani (white arrow). Additional smaller prostate tumors are highlighted on the diffusion-weighted images (white arrowheads). At biopsy, pathology revealed prostate cancer in 12 out of 12 cores with thw highest Gleason score of 5 + 4 and maximum percentage of cancer core of 100%

the detection of EPE and SVI, with especially improved performance in the assessment of SVI [61].

Active surveillance

The widespread use of screening for prostate cancer using the measurement of serum PSA levels has resulted in the increased detection (Fig. 3) and treatment of cases of low-grade and low-volume cancer, estimated as between 25–50% of newly diagnosed cases [62]. This has led to wider acceptance and adoption of active surveillance, targeted at low-risk prostate cancers where the patient undergoes a protocol-based surveillance strategy without treatment until there is evidence of clinical or radiological progression. This aims to reduce the drawbacks of overdiagnosis and overtreatment of clinically indolent tumors and at the same time avoid unwanted side effects of more radical treatments such as radiotherapy, ablative therapy, and radical prostatectomy as theoretically these tumors will not lead to cancer-related mortality and morbidity during the patients' life expectancy. Although there is an increasing relaxation of enrolling patients into active surveillance programs, it is recommended by the National Comprehensive Cancer Network (NCCN) for men who meet the following definition of very low-risk prostate cancer: clinical stage ≤T1c, Gleason score ≤ 6; <3/12 benign cores on biopsy; <50% of cancer-positive tissue in each biopsy core; PSA <10 ng/ml, and >20 years of life expectancy [63]. Other guidelines such as those by the European Association of Urology (EAU) are similar in terms of their inclusion criteria with mild variation in details [64]. After being included in an AS protocol, the patients are recommended to undergo a follow-up protocol. For example, according to the NCCN guidelines: PSA every six months, a DRE every 12 months, and a re-biopsy every 12 months if there are no earlier clinical indications [63]. Cancer progression can be detected by increasing PSA (>10 ng/ml) and Gleason score of ≥7 in repeat biopsy, however as of now imaging progression on MRI is not included as a criterion for progression during active surveillance [53, 54].

Although clinical and pathological information have traditionally been the basis of active surveillance, integration of MRI findings has been increasingly proposed [65–67]. For instance, the European Association of Urology (EAU) guidelines recommend mpMRI for patients on active surveillance prior to a confirmatory biopsy or even the initial biopsy [68]. This is especially relevant for tumors that are located in the anterior prostate which account for 20% [69, 70], as they are often missed on systematic randomized biopsies and even when biopsied, are not so rarely underestimated with having fewer positive cores containing cancerous tissue and shorter core lengths: median biopsy core length of 8 mm vs 1 mm using targeted systematic biopsy

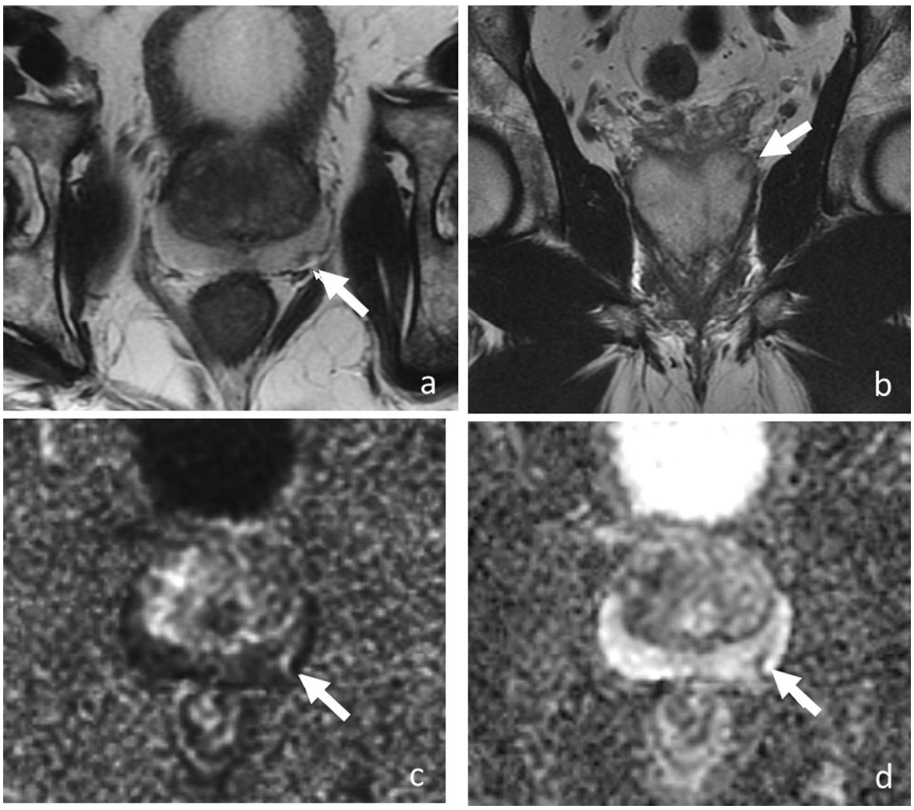

Fig. 3 Axial T2-weighted images (**a**,**b**), DWI (**c**), and ADC (**d**). MRI of 73-year-old man with PSA level of 3.77 ng/ml shows 0.5-cm lesion (arrow) in the left posterior base peripheral zone demonstrating hypointense T2 signal on axial (**a**) and coronal plane (**b**). Lesion has marked diffusion restriction (image **c**,**d**) and was reported as PI-RADS v2 score of 4. Transrectal ultrasound-guided biopsy revealed low-volume Gleason 3 + 4 prostate cancer. For 8 years, patient has been on active surveillance without clinical or radiological progression

versus non-targeted biopsy [69, 70]. In patients that were enrolled in active surveillance programs based on a negative prior 12-core transrectal US-guided biopsy, the percentage of those with cancer of the anterior portion of the gland indicated as a suspicious lesion on MRI and diagnosed with a targeted biopsy was high, at up to 89% [71]. Regardless of the location (anterior vs posterior), MRI has the advantage of targeting suspicious lesions for biopsies [69] and achieving better risk stratification based on a more accurate assessment of tumor volume and grade [69]. MRI-Tb can be done using either cognitive fusion [72] or software-based MRI/TRUS fusion [73], and even in-bore direct MRI-guided biopsies [74, 75].

In addition to MRI being increasingly used to detect clinically significant disease missed during initial biopsy or to prevent the need for a second biopsy [76], there is more evidence demonstrating the association between stability on MRI and stability of the Gleason score on follow-up biopsies during active surveillance [77]. However, the potential role and timing of MRI in this field remains to be determined in clinical practice owing to the heterogeneity of the inclusion criteria for active surveillance patients, the definition of clinically significant disease, and agreement regarding the definition of radiologic progression [78]. To address these issues, recently an international consensus panel proposed a standardized reporting scheme for patients undergoing follow-up MRI during active surveillance, namely the Prostate Cancer Radiological Estimation of Change in Sequential Evaluation (PRECISE) recommendations [79]. PRECISE guidelines facilitate the building of an evidence archive for tracking prostate MRI results over time in men under active surveillance taking into account measurement error inter-scan technical acquisition variability on MRI, and in turn identify "true" radiological progression by providing a score between 1–5. Although it is unknown whether this will be integrated into clinical practice, early studies show promising results where PRECISE scores of ≥4 have very high negative predictive values of 0.96 for progression on biopsy [80] which can serve as evidence to integrate MRI in follow-up protocols for patients on active surveillance.

Treatment planning

MRI of the prostate can assist treatment planning in several ways. With regards to surgery, prostate cancer patients without a high risk of EPE are typically offered a nerve-preserving radical prostatectomy which comes with the advantage of reducing unwanted postsurgical complications such as erectile dysfunction and urinary incontinence [81]. However, nerve-preserving approaches are associated with potential positive margins, which introduce risk for recurrence and therefore accurate prediction of EPE is required to properly plan for radical surgery in terms of whether to perform nerve-preserving approaches or not [82]. Traditionally available prediction methods including DRE, transrectal ultrasound, and clinical nomograms based on factors such as PSA are suboptimal. Therefore, all available tools need to be used before treatment for evaluating the benefits and hazards of nerve-sparing techniques and developing treatment plans specific to each patient [83]. MRI has a great advantage in this area by being able to detect and localize the dominant lesion and by assessing its relationship with the neurovascular bundle (NVB). For example, the dominant lesion may be organ-confined, extending to the capsule, or demonstrating frank extracapsular extension with involvement of the NVB. Many prior studies have assessed the ability of MRI to help plan whether to preserve or resect the NVB. According to Schiavina et al. [84], using mpMRI altered the nerve-sparing strategy in approximately half of the cases and it was deemed that in 75% of the cases, the changes in strategy were appropriate. In addition, Panebianco et al. [85], reported that preoperative mpMRI supports the surgeon in selecting the appropriate surgical technique and may improve the quality of the excision in up to 96% of the patients. Nevertheless, careful consideration of risk factors such as older age or higher Gleason grade should be considered, as such has been reported to be associated with intra-operative aborting of a preoperatively planned nerve-sparing strategy [86].

MRI has also become helpful for planning radiation treatment owing to several of its advantages when compared with CT, the more conventional anatomical imaging used for treatment planning. Not only does MRI help directly visualize the tumor, but also its superior soft-tissue resolution and anatomical detail allow for better involvement of the prostatic apex and the presence of EPE and SVI which are crucial for determining the radiation dose and field [87]. More recent investigations are attempting to see whether adding focal boost doses to the macroscopically visible dominant tumor on MRI results in better outcomes where a phase III randomized trial showed that it improves biochemical disease-free survival without increased toxicity [88].

MRI is also increasingly being used related to focal ablative therapies, specifically with regards to patient selection, treatment planning, and intra-procedural monitoring, usually in the setting of a clinical trial. MRI can assist in determining several important factors such as bilaterality, localization, size, and extent (e.g., EPE or SVI) to determine eligibility and whether to perform partial vs total gland ablation [89]. During the ablation process, MR thermometry can then be used for real-time monitorng of the thermal destruction [90].

Role of imaging in biochemical recurrence

The definition of biochemical recurrence (BCR) after a curative treatment for prostate cancer relies on the initial treatment given to the patient. Although there are several definitions for BCR, a commonly used one in the setting of radical prostatectomy is defined as PSA value of ≥0.2 ng/ml confirmed by a subsequent PSA value of ≥0.2 ng/ml. After radiotherapy, a rise of 2 ng/mL or more above the nadir PSA is considered as BCR; the PSA nadir being the lowest level of the PSA reached after the treatment and usually occurring within the first year after the treatment but may occur within 18 to 30 months [91, 92].

The role of imaging in the context of BCR is to determine whether it represents local or metastatic disease, and ideally to detect the disease as early as possible at a lower level of PSA to help determine the optimal management (e.g., salvage radiation treatment in patients that underwent prostatectomy or systemic treatment) [91, 93]. MpMRI of the pelvis currently plays a role in this setting as it provides superior soft-tissue resolution and anatomical detail of anatomical sequences (e.g., T2WI) when compared with CT and by utilizing advanced functional sequences (e.g., DWI and DCE-MRI) enabling detection of locally recurrent disease in the setting of BCR [91]. In addition, when performed together with whole-body MRI, this allows detection and quantification of distant metastases (e.g., differentiation of oligometastatic from polymetastatic disease), including bones, lymph nodes and soft tissues, and to potentially guide management.

Also, in relation to BCR MRI is increasingly being investigated as a prognostic tool to predict BCR prior to definitive local therapy. A recent systematic review and meta-analysis showed that higher PI-RADS v2 scores were associated with increased risk of BCR predominantly in the context of radical prostatectomy [94]. Few studies also show that these prognostic values translate into higher-level oncological outcomes (e.g., metastasis and cancer-specific mortality) when interrogating MRI that were used prior to the introduction of "PI-RADS" and with long-term follow-up (median follow-up around 10 years) [95, 96]. Similar prognostic value for BCR and other oncological outcomes have been reported in the context of radiation treatment [87].

Local recurrence after radical prostatectomy

Common mpMRI findings and pitfalls

The most frequent location of local recurrence following radical prostatectomy is the vesicourethral anastomosis, followed by the anterior or posterior bladder neck [97]. It typically manifests as intermediate T2 signal intensity with early enhancement and restricted diffusion [97, 98] (Fig. 4). Susceptibility artifacts from surgical clips can limit evaluation, especially on DWI [97]. The role of the radiologist includes being familiar with common pitfalls that include postsurgical fibrosis, residual prostate or seminal vesicles

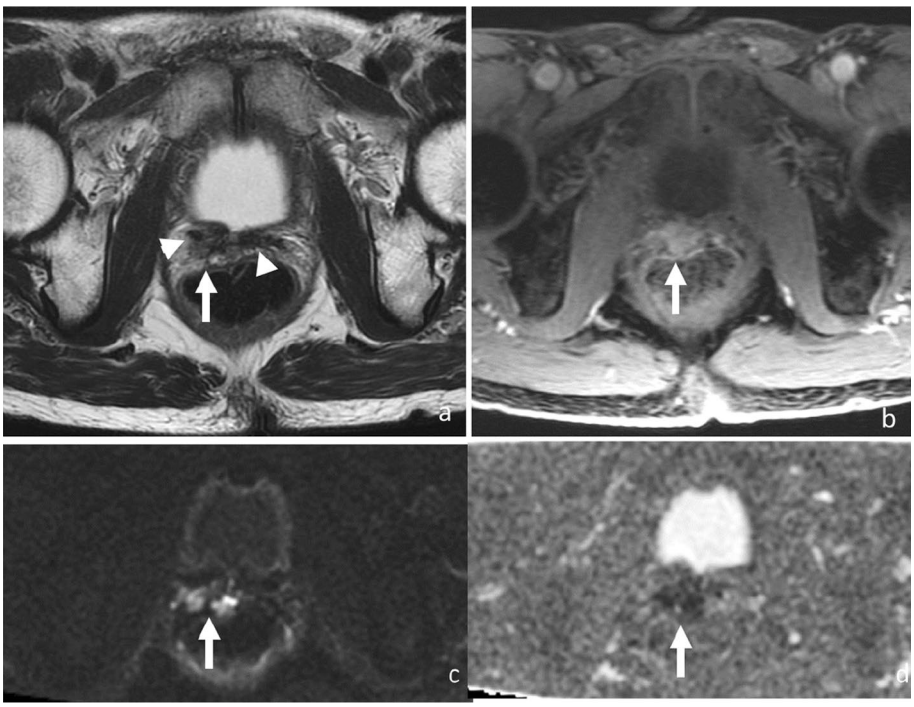

Fig. 4 Axial T2-weighted (**a**), DCE (**b**), DWI (**c**) and ADC (**d**). 68-year-old man with rising PSA (5.78 ng/ml) 6 years after radical prostatectomy for Gleason score 4 + 4 prostate cancer. MRI shows a 2.2-cm T2 intermediate signal mass (arrow) in the right prostatectomy bed scar tissue demonstrating T2 low signal (arrowheads). Mass shows early enhancement and restricted diffusion. Patient was started on androgen deprivation therapy after which both this recurrent tumor on MRI and PSA levels decreased

[97, 99]. Postsurgical fibrosis usually shows a delayed and progressive enhancement, T2 hypointense signal, and lack of restricted diffusion [97, 98]. Residual prostatic tissue is problematic as PSA will remain detectable due to normal functional prostate tissue and even clinically false considered to be "PSA failure" after prostatectomy. Although they tend to maintain location and imaging features similar to pretreatment prostate, differentiation with recurrent tumor is difficult [97]. Most commonly, with residual prostate gland tissue, PSA does not drop to undetectable levels after the surgery [97]. Remnant seminal vesicles are identified up to 20% of cases and can be easily characterized by their convoluted appearance [98, 100]. An important drawback is that detection of recurrent tumor after prostatectomy depends on the PSA level, for example only 11% patients had positive findings on MRI in patients with PSA less than 1 ng/ml [101].

Performance of MRI for local recurrence

The diagnostic performance of MRI for detecting local recurrence varies with sensitivities and specificities ranging from 48 to 100% and 52% to 100%, respectively, depending on the combination of MRI sequences used and the patient population [102, 103]. DCE-MRI is the most valuable sequence for evaluation of biochemical recurrence after prostatectomy, with higher sensitivity and specificity (87–100% and 94%, respectively) when compared to T2W or DWI alone [104, 105] and this can be improved by using a combination of DCE-MRI and T2WI [92, 104, 106–109]. Panebianco et al. found that the overall accuracy of the combination DCE + T2WI was superior to the combination DWI + T2W [106]. Although DWI is commonly hampered by artifacts from surgical clips, it increases the conspicuity of recurrent tumors, helping avoid pitfalls such as misdiagnosing peri-prostatic vessels as enhancing nodules in addition to enhancing detection of nodal and bone metastases when image quality is sufficient [92, 106]. Therefore, under optimal conditions, a mpMRI protocol consisting of T2-weighted imaging, DCE-MRI, and DWI may provide the best diagnostic performance [107].

DCE Semiquantitative, quantitative, and automated detection

Semiquantitative and quantitative DCE analyses have been extensively evaluated in the postoperative setting of BCR. Examples of semiquantitative parameters are peak enhancement, time to peak, washout slope, area under the contrast enhancement curve, and quantitative parameters include *K*trans, V*e*, and *K*ep [104, 110]. Most of the local recurrences after prostatectomy demonstrate early enhancement with rapid or plateau/slow washout after intravenous contrast administration (44% and 50%, respectively) [111]. Investigators have also developed automated software for the detection and delineation of suspicious lesions in the prostate bed using DCE-MRI [112].

MRI findings after radiotherapy and local recurrence

Common mpMRI findings and pitfalls

Radiotherapy causes atrophy, inflammation, and fibrosis, which manifests as a smaller, diffusely T2 hypointense prostate gland with decreased contrast between the treated tumor and the background prostate tissue on MRI [98]. Recurrent tumor after radiotherapy most frequently is located at the site of the treated initial tumor, therefore, it is crucial for the radiologist to take into account the pre-treatment imaging studies where available [98]. If the patient has received low-dose-rate brachytherapy, the seeds typically appear as small-signal voids scattered throughout the gland, causing susceptibility artifacts and hampering the performance of DWI. This is not the case for high-dose-rate brachytherapy since no permanent seeds are implanted. Local recurrence usually manifests with restricted diffusion and early enhancement. Postradiation inflammatory changes can also mimic these findings leading to false-positive interpretations; hence caution is warranted for performing MRI within the first three months [98].

Performance of mpMRI sequences

Usage of functional MRI sequences are crucial in the radiologist's perspective for detecting recurrent tumor after radiation treatment (Fig. 5). In a meta-analysis by Wu et al. [103], DCE imaging significantly increased the sensitivity and specificity of MRI when compared to T2W alone (sensitivity and specificity 60–97% and 64–93% for T2W + DCE versus 39–85% and 51–88% for T2W alone, respectively). In addition, Donati et al. [113] reported that DWI with T2W imaging was superior to T2W imaging alone. Using a full mpMRI with DWI, DCE-MRI and T2WI to further improve detection has been controversial; for example, Roy et al. [104] found that all three sequences resulted in high accuracy in identifying recurrence (e.g., sensitivity of 100%), whereas Donati et al. did not observe any benefit of adding DCE-MRI to DWI and T2WI [113].

ADC values

Studies have reported a correlation between ADC values and treatment response after radiotherapy, suggesting that ADC value may be helpful as an imaging biomarker for

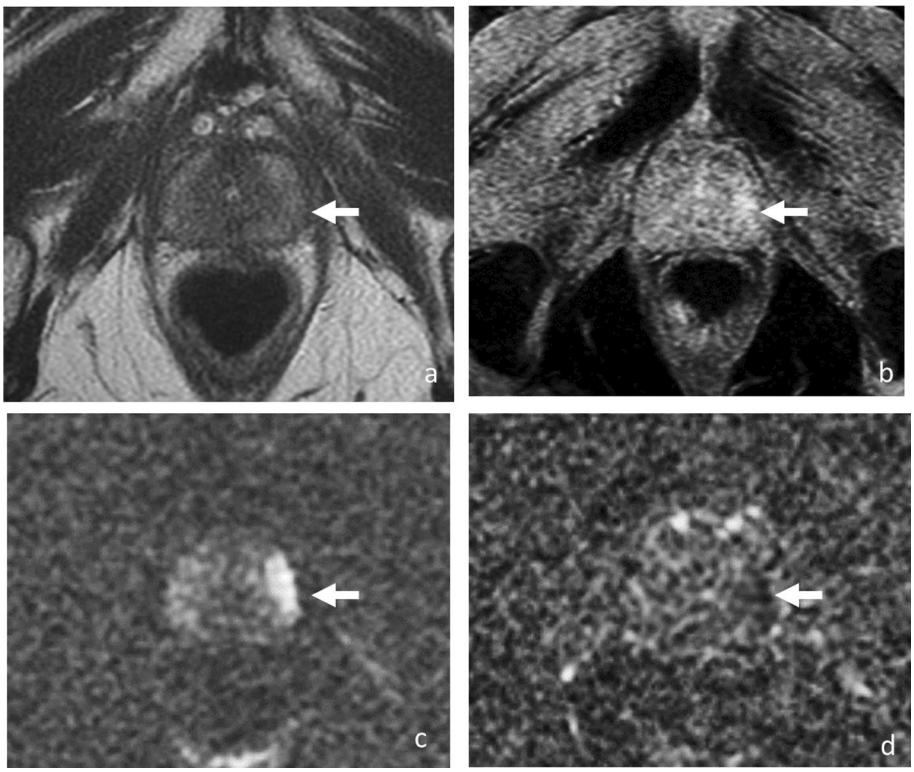

Fig. 5 Axial T2-weighted image (**a**), DCE (**b**), DWI (**c**) and ADC (**d**). 64-year-old man with rising PSA biochemical recurrence (3.59 ng/ml) after external beam radiotherapy to a Gleason 3 + 3 prostate cancer 14 years ago. Diffuse low T2 signal throughout the entire prostate and loss of zonal differentiation represent post-treatment changes, limiting detection of recurrent tumor. However, 1.6-cm focal lesion (arrow) in the left mid gland peripheral zone is demonstrated on early DCE images and diffusion-weighted images which was confirmed on biopsy as Gleason 4 + 4 cancer

monitoring the therapeutic response and identifying a recurrence of prostate cancer. For example, tumor ADC values increase when compared to pretreatment values, while that in the benign prostate tissue decrease, ultimately making treated tumor indistinct [114, 115]. Pasquier et al. [116] demonstrated that early ADC changes correlated with late PSA decrease for patients treated by external beam radiation treatment. Morgan et al. [117] have shown that an ADC was useful in detecting local tumor recurrence larger than 0.4 cm^2, with a cutoff ADC of 1216×10^{-6} mm^2/s showing sensitivity and specificity of 100% and 96%, respectively.

Radiomics after radiotherapy

Radiomics have been shown to be a potential biomarker in the context of radiotherapy response assessment. Lee et al. [118] reported that first and second-order features of gross tumor volume and prostate utilizing T2WI and ADC map have significant changes during radiotherapy; for example, an increase of tumor ADC mean and reduction of entropy and contrast on ADC map were observed, probably representing a reduction on tumor cellularity and heterogeneity. Whether this will translate into clinical practice, in the radiologists' perspective, will require validation and standardization.

MRI findings after focal therapies

Focal therapies, including cryotherapy, high-intensity focused ultrasound, and photodynamic therapy, have increasingly been used as an alternative treatment for low and intermediated risk, organ-confined prostate cancer to avoid common morbidities associated with standard radical therapies (e.g., prostatectomy and radiotherapy) [119]. Focal therapies treat the tumor through necrosis via their own specific mechanism, therefore, manifesting with expected MRI findings of a non-enhancing area at the site of the treated tumor [120]. Tumor recurrence typically appears as an early enhancing focal lesion with restricted diffusion in or adjacent to this region as T2WI offers limited information due to architectural distortion and other post-treatment changes [121, 122] (Fig. 6).

MRI findings after androgen-deprivation therapy (ADT) and local recurrence

ADC values

Radiologists may play a critical role in response assessment after neoadjuvant ADT prior to prostatectomy or

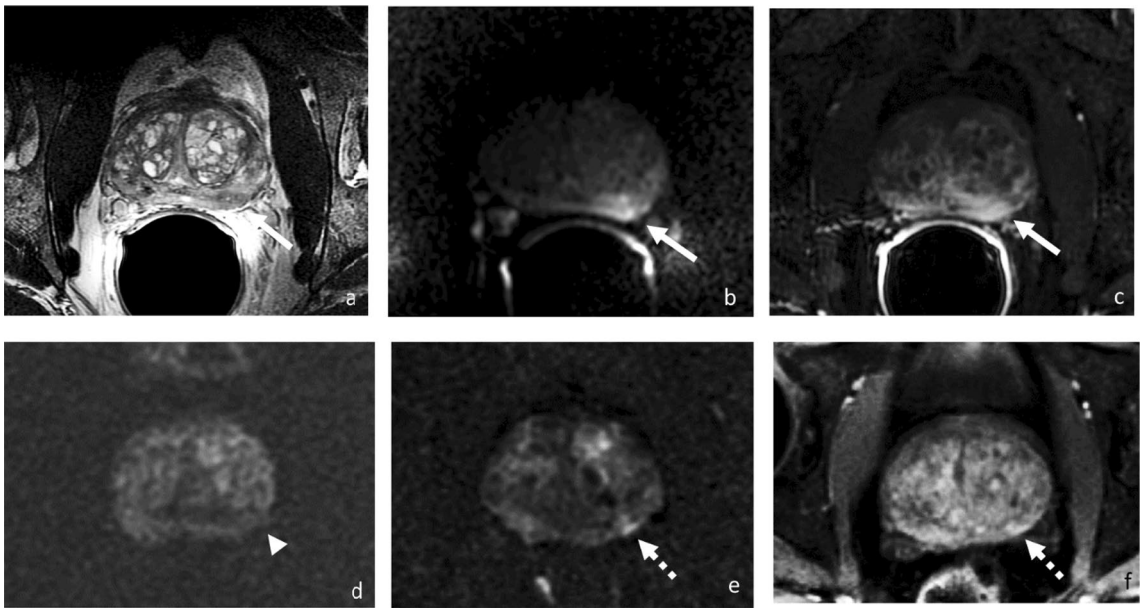

Fig. 6 Axial T2-weighted (**a**), DWI (**b**) and DCE-MRI (**c**) before, DWI (**d**) 3 months after, and DWI (**e**) and DCE-MRI (**f**) 2 years after focal therapy, respectively. 63-year-old patient with PSA 5.8 ng/ml and a left mid gland peripheral zone lesion at presentation for which biopsy showed Gleason 3 + 4 prostate cancer. Three months after irreversible electroporation (IRE), there was no abnormal signal on DWI at the site of the treated tumor (arrowhead). Two years after IRE with PSA rose to 10.76 ng/ml, and MRI demonstrated a lesion (broken arrow) adjacent to the ablation site demonstrating early enhancement and restricted diffusion suspicious for recurrence that was confirmed by biopsy

radiation treatment [123]. In addition to changes in serum PSA levels, MRI is able to provide additional information regarding treatment response during ADT including changes in terms of prostate size and tumor volume. Moreover, investigators have also noted a correlation between ADC value in the tumor and treatment response [124–126]. Kim et al. [124] described that the mean ADC value of tumors (1060×10^{-6} mm^2/s) was significantly increased after treatment when confronted with the pre-treatment values (780×10^{-6} mm^2/s), and that increasing trend was negatively correlated with decreasing PSA. Further studies are needed if this will help predict pathological downstaging or even pathological complete response.

DCE

DCE has also shown potential for assessing treatment response to ADT. Padhani et al. [24] observed a reduction in tumor permeability and washout patterns and found that this coincided with a PSA decline in 91% of the patients on ADT. In addition, this can be semi-quantitatively assessed, for example, enhancement slopes with a slow progressive rise in enhancement were seen in most post-treatment cases in contrast to early enhancement followed by plateau or washout on pre-treatment imaging [127]. Quantitative parameters such as tumor blood volume have also been shown to capture treatment response [128].

Radiomics

Although morphological and functional imaging can be used to assess response to ADT, diffuse signal changes and decreased conspicuity between the treated tumor and background prostate may limit evaluation. Radiomics has been suggested as a supporting tool to discriminate the tumor from normal tissue, especially in radiotherapy planning after a neoadjuvant ADT therapy. First-order texture features using ADC were significantly different between tumor and normal tissue after ADT [129]. Daniel et al. [125] reported that ADC and T2WI textural features performed better in discriminating healthy from tumor tissue when compared to the simple histogram parameters in patients treated with ADT.

Prostate imaging for recurrence reporting (PI-RR)

Recently, a structured reporting scheme called Prostate Imaging for Recurrence Reporting (PI-RR) was proposed for the purpose of standardizing acquisition, interpretation, and reporting of MRI for evaluating local recurrence of prostate cancer [98]. PI-RR uses a 5-point scoring system to determine the probability of relapse on MRI where scores of 1 and 5 are given to lesions with a very low and very

high likelihood of recurrence). This system relies on anatomical and functional imaging findings based on the exiting large body of evidence that has accumulated until today and approaches differently for each different type of treatment the patient had received. Anatomical parameters include the size, location, and shape of the lesion, while functional criteria correspond to findings on DWI and DCE [98].

Metastatic prostate cancer

Currently, Tc-99 m bone scintigraphy (BS) and computerized tomography (CT) are most widely used to assess bone metastases despite their well-recognized limited sensitivity, because of their wide availability and recognized associations with prognosis [130]. These modalities commonly show "flare phenomena" during treatment where the metastatic lesions demonstrate increased radionuclide uptake on BS which can be falsely misinterpreted as progression [131, 132]. MRI along with PET/CT on the other hand, has the potential to identify changes in the bone marrow before osteoblastic response [91]. PET/CT, especially when used with certain radioisotopes such as PSMA-targeted ones, has been extensively shown to be superior to conventional imaging techniques for detecting metastatic disease [133–135]. MRI in the form of whole-body imaging, although less extensively investigated has shown promising results in addition to its unique advantage of avoiding radiation exposure [136, 137]. Furthermore, performing whole-body MRI together with mpMRI of the pelvis allows a "one-stop-shop" approach for primary staging in high-risk patients and in the setting of biochemical recurrence, offering an assessment of both local and distant metastases [136].

Whole-body MRI

Whole-body MRI has shown good performance in detecting bone metastases [138]. Studies have found that whole-body MRI performs better than bone scintigraphy and is similar to ^{18}F-choline PET/CT [137, 139, 140]. A study showed an AUC of 0.971 using a combination of T1WI + T2WI + short tau inversion recovery + DWI vs AUC 0.943 just using T1WI + T2WI + DWI for detecting bone metastases when compared to ^{18}F-choline PET/CT [137]. A meta-analysis performed by Shen et al. [141] found that whole-body MRI had a higher sensitivity and AUC than choline PET/CT in detecting bone metastasis on a per-patient analysis (95% and 0.987 versus 87% and 0.954, respectively), with similar specificity (96% for whole-body MRI versus 97% for choline PET/CT). Although similar overall per-patient sensitivity of detecting patients with bone metastases have been suggested using routine mpMRI of the prostate and whole-body MRI, the latter has the advantages of superior per-lesion detection rate and therefore the potential for selecting patients with oligometastatic disease (Fig. 7) which could be amenable for metastasis-directed therapy such as stereotactic body radiation therapy [131, 132]. In addition, quantification of metastatic burden can be done with whole-body MRI may also be a prognostic factor, using quantitative automated software, which can be used to assess treatment response and obtain prognostic information. For example, Perez-Lopez et al. [142] demonstrated a correlation between the volume of bone metastasis quantified on whole-body DWI in metastatic castrate resistance prostate cancer, overall survival, and other already established prognostic biomarkers (e.g., PSA and hemoglobin).

Assessment of therapy response of bone metastases has been reported to be done using changes in ADC values (e.g., increase when responding to ADT) [143]. Texture analysis may provide additional information such as the correlation between changes of first-order (e.g., kurtosis, energy, and entropy) and second-order metrics (e.g., contrast and homogeneity and changes in PSA across time [144]. Additional studies are needed to verify these findings.

MRI has not shown satisfactory performance regarding discrimination of lymph node metastasis as it relies on morphologic criteria such as size and shape, not being able to detect microscopic metastases within the lymph nodes, and false-positive interpretation of enlarged reactive lymph nodes similar to CT [145]. The pooled sensitivity and specificity of MRI for detecting pelvic nodal metastasis were 53% and 95%, respectively, in a recent meta-analysis [146, 147]. Although DWI is a great sequence to detect lymph nodes, its role in differentiating benign from malignant lymph nodes is controversial [148–150]. Usage of ultra-small super paramagnetic iron oxide (USPIO) has shown in several studies to improve sensitivity, rendering it superior to CT, potentially allowing detection of metastases even in normal-sized lymph nodes, and also to play a complementary role to PSMA PET/CT (which currently allows for the best detection rate) [151–153]. Nevertheless, several obstacles such as iron overload and availability need to be addressed before the widespread adoption of this promising technique.

MET-RADS-P

The METastasis Reporting and Data System for Prostate Cancer (MET-RADS-P) were recently created to improve standardization and reduce variations in the acquisition, interpretation, and reporting of whole-body MRI in advanced prostate cancer [154]. On MET-RADS-P, DWI evaluation is based on subjective comparison of the signal intensity on high b-value DWI to adjacent muscle signal intensity. In contrast, ADC is quantitatively assessed based on their values (10^{-3}mm^2/s). According to the MET-RADS-P, measurements of bone lesions should be undertaken on

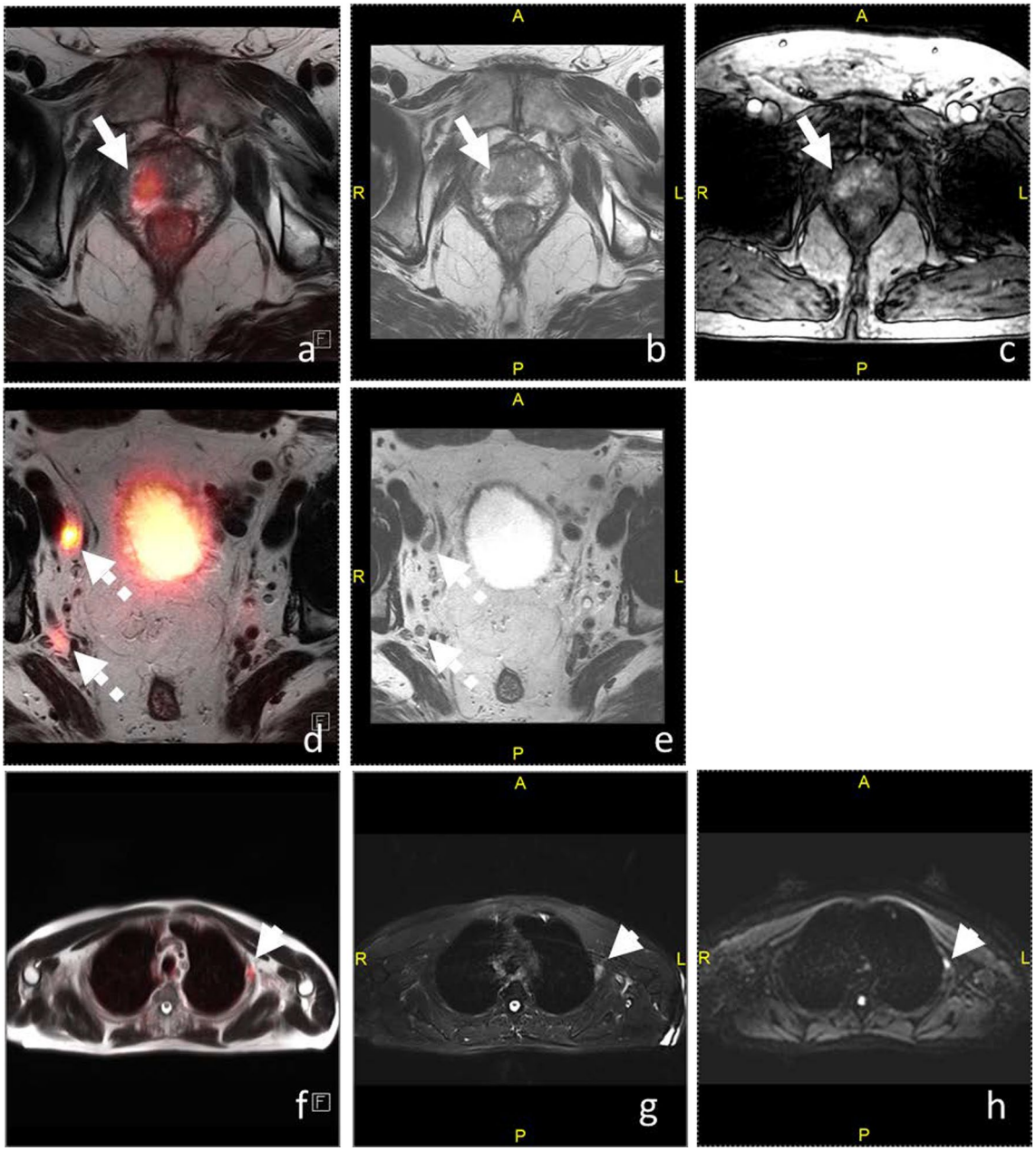

Fig. 7 Fused axial T2WI/PSMA-PET (**a**), axial T2WI (**b**), and axial DCE-MRI (**c**) of the prostate, fused axial T2WI/PSMA-PET (**d**) and axial T2WI (**e**) of the pelvic lymph nodes, and fused axial T2WI/PSMA-PET (**f**), axial fat-suppressed T2WI (**g**), and axial DWI (**h**) of the thorax. 79-year-old man with PSA of 8.0 ng/ml had Gleason 4 + 3 prostate cancer on biopsy. (**a**–**c**) Right apical peripheral zone T2 hypointense lesion is PSMA-avid (SUV 23.0) with early enhancement. (**d**–**e**) Right external (1.3 × 0.8 cm; SUV 86.6) and internal iliac lymph nodes (0.7 × 0.6 cm, rounded in shape; SUV 12.8) are suspicious for metastases. (**f**–**h**) Lateral left 3rd rib lesion demonstrates PSMA avidity (SUV 7.2) and restricted diffusion which was confirmed as metastasis on biopsy

high-quality T1WI. They advocate the record of up to five discrete bone lesions with at least one lesion in the appendicular skeleton if present, up to five discrete lymph nodes, and up to five soft tissue lesions (15 lesions maximum), all of them should measure at least 1.5 cm. On follow-up scans, changes in the metastases should be assessed and recorded at a regional level. Then, the status of the primary disease, nodes, viscera, and bone disease should be registered separately using the overall response assessment template form.

PET/MRI

Integrated or simultaneous PET/MRI is an emerging technology that combines PET images with concurrent or

consecutive whole-body MRI. The novelty of this technology in evaluating patients with prostate cancer stands in the combination of the benefits of MRI for local and distant disease as described above and the functional information provided by PET using tracers such as ^{11}C-choline, ^{18}F-fluciclovine, or PSMA-targeted radioligands (Fig. 7) [97]. Studies have shown that using integrated PET/MRI as opposed to PET/CT alone using these radioligands, may provide better localization and anatomic characterization especially for locally recurrent tumors in the prostate bed, which may be difficult to assess especially in urinary excreted PSMA agents [155]. Galgano et al. [156] demonstrated that ^{18}F-fluciclovine PET/MRI detected suspected metastatic lymph nodes in 50% of patients that were not enlarged (short axis < 1.0 cm). Souvetzoglou et al. [157] found that ^{11}C-choline PET/MRI had similar performance than PET/CT in detecting choline-positive bone metastases; however, PET/MRI showed better anatomical localization of lesions. However, the optimal target population and the true incremental value in performing the PET/MRI in an integrated/simultaneous manner instead of a prostate MRI + PET/CT has not been established and will need to be investigated in future studies.

Conclusion

There has been increased utilization of MRI in various aspects of prostate cancer management over the recent years. While MRI has already been integrated as a key imaging modality in many clinical settings, emerging MRI techniques are promising for increasing precision and allowing for expanding the role of MRI.

Funding This study was funded in part through the NIH/NCI Cancer Center Support Grant P30 CA008748.

Declarations

Conflicts of interest Since May 2017, Dr. Hricak has served on the Board of Directors of Ion Beam Applications (IBA), a publicly traded company, and she receives annual compensation for her service. Furthermore, Dr. Hricak is a member of the External Advisory Board of the Sidney Kimmel Comprehensive Cancer Center at Johns Hopkins (SKCCC), the International Advisory Board of the University of Vienna, Austria, the Scientific Committee of the DKFZ (German Cancer Research Center), Germany, the Board of Trustees the DKFZ (German Cancer Research Center), Germany and a member of the Scientific Advisory Board (SAB) of Euro-BioImaging ERIC; she does not receive financial compensation for any of these roles. The other authors of this manuscript declare no relationships with any companies, whose products or services may be related to the subject matter of the article.

Research involving human participants and/or animals This article does not contain any studies with human participants performed by any of the authors.

Informed consent Informed consent for this review article was waived regarding all individual participants included in the study.

References

1. Verma S, Rajesh A (2011) A clinically relevant approach to imaging prostate cancer: review. AJR Am J Roentgenol 196(3 Suppl):S1-10
2. Glazer DI, Davenport MS, Khalatbari S, Cohan RH, Ellis JH, Caoili EM et al (2015) Mass-like peripheral zone enhancement on CT is predictive of higher-grade (Gleason 4 + 3 and higher) prostate cancer. Abdom Imaging 40(3):560–570
3. Ahmed HU, El-Shater Bosaily A, Brown LC, Gabe R, Kaplan R, Parmar MK et al (2017) Diagnostic accuracy of multi-parametric MRI and TRUS biopsy in prostate cancer (PROMIS): a paired validating confirmatory study. Lancet 389(10071):815–822
4. Woo S, Ghafoor S, Vargas HA (2019) Contribution of radiology to staging of prostate cancer. Semin Nucl Med 49(4):294–301
5. Woo S, Suh CH, Kim SY, Cho JY, Kim SH, Moon MH (2018) Head-to-head comparison between biparametric and multiparametric mri for the diagnosis of prostate cancer: a systematic review and meta-analysis. AJR Am J Roentgenol 211(5):W226–W241
6. Abreu-Gomez J, Lim C, Cron GO, Krishna S, Sadoughi N, Schieda N (2021) Pharmacokinetic modeling of dynamic contrast-enhanced (DCE)-MRI in PI-RADS category 3 peripheral zone lesions: preliminary study evaluating DCE-MRI as an imaging biomarker for detection of clinically significant prostate cancers. Abdom Radiol 2:2
7. Bae H, Cho NH, Park SY (2019) PI-RADS version 2: optimal time range for determining positivity of dynamic contrast-enhanced MRI in peripheral zone prostate cancer. Clin Radiol 74(11):895
8. Park SY, Park BK, Kwon GY (2020) Diagnostic performance of mass enhancement on dynamic contrast-enhanced MRI for predicting clinically significant peripheral zone prostate cancer. AJR Am J Roentgenol 214(4):792–799
9. Woo S, Suh CH, Kim SY, Cho JY, Kim SH (2017) Diagnostic performance of prostate imaging reporting and data system version 2 for detection of prostate cancer: a systematic review and diagnostic meta-analysis. Eur Urol 72(2):177–188
10. Westphalen AC, McCulloch CE, Anaokar JM, Arora S, Barashi NS, Barentsz JO et al (2020) Variability of the positive predictive value of PI-RADS for prostate MRI across 26 centers: experience of the society of abdominal radiology prostate cancer disease-focused panel. Radiology 296(1):76–84
11. Seetharam Bhat KR, Samavedi S, Moschovas MC, Onol FF, Roof S, Rogers T et al (2021) Magnetic resonance imaging-guided prostate biopsy-a review of literature. Asian J Urol 8(1):105–116
12. Woo S, Suh CH, Eastham JA, Zelefsky MJ, Morris MJ, Abida W et al (2019) Comparison of magnetic resonance imaging-stratified clinical pathways and systematic transrectal ultrasound-guided biopsy pathway for the detection of clinically significant prostate cancer: a systematic review and meta-analysis of randomized controlled trials. Eur Urol Oncol 2(6):605–616
13. Kasivisvanathan V, Rannikko AS, Borghi M, Panebianco V, Mynderse LA, Vaarala MH et al (2018) MRI-targeted or standard biopsy for prostate-cancer diagnosis. N Engl J Med 378(19):1767–1777

14. Eklund M, Jäderling F, Discacciati A, Bergman M, Annerstedt M, Aly M et al (2021) MRI-targeted or standard biopsy in prostate cancer screening. N Engl J Med 2:2
15. Borofsky S, George AK, Gaur S, Bernardo M, Greer MD, Mertan FV et al (2018) What are we missing? False-negative cancers at multiparametric MR imaging of the prostate. Radiology 286(1):186–195
16. Padhani AR, Barentsz J, Villeirs G, Rosenkrantz AB, Margolis DJ, Turkbey B et al (2019) PI-RADS steering committee: the PI-RADS multiparametric MRI and MRI-directed biopsy pathway. Radiology 292(2):464–474
17. Chaddad A, Kucharczyk MJ, Niazi T (2018) Multimodal radiomic features for the predicting Gleason score of prostate cancer. Cancers (Basel) 10:8
18. Chaddad A, Niazi T, Probst S, Bladou F, Anidjar M, Bahoric B (2018) Predicting Gleason score of prostate cancer patients using radiomic analysis. Front Oncol 8:630
19. Liu L, Tian Z, Zhang Z, Fei B (2016) Computer-aided detection of prostate cancer with MRI: technology and applications. Acad Radiol 23(8):1024–1046
20. Peng Y, Jiang Y, Antic T, Giger ML, Eggener SE, Oto A (2014) Validation of quantitative analysis of multiparametric prostate MR images for prostate cancer detection and aggressiveness assessment: a cross-imager study. Radiology 271(2):461–471
21. Wang S, Burtt K, Turkbey B, Choyke P, Summers RM (2014) Computer aided-diagnosis of prostate cancer on multiparametric MRI: a technical review of current research. Biomed Res Int 2014:789561
22. Bardis MD, Houshyar R, Chang PD, Ushinsky A, Glavis-Bloom J, Chahine C et al (2020) Applications of artificial ıntelligence to prostate multiparametric MRI (mpMRI): current and emerging trends. Cancers (Basel). 12:5
23. Mortensen MA, Borrelli P, Poulsen MH, Gerke O, Enqvist O, Ulen J et al (2019) Artificial intelligence-based versus manual assessment of prostate cancer in the prostate gland: a method comparison study. Clin Physiol Funct Imaging 39(6):399–406
24. Strom P, Kartasalo K, Olsson H, Solorzano L, Delahunt B, Berney DM et al (2020) Artificial intelligence for diagnosis and grading of prostate cancer in biopsies: a population-based, diagnostic study. Lancet Oncol 21(2):222–232
25. Goldenberg SL, Nir G, Salcudean SE (2019) A new era: artificial intelligence and machine learning in prostate cancer. Nat Rev Urol 16(7):391–403
26. Raciti P, Sue J, Ceballos R, Godrich R, Kunz JD, Kapur S et al (2020) Novel artificial intelligence system increases the detection of prostate cancer in whole slide images of core needle biopsies. Mod Pathol 33(10):2058–2066
27. Sunoqrot MRS, Selnaes KM, Sandsmark E, Nketiah GA, Zavala-Romero O, Stoyanova R et al (2020) A quality control system for automated prostate segmentation on T2-weighted MRI. Diagnostics 10:9
28. Khalvati F, Zhang J, Chung AG, Shafiee MJ, Wong A, Haider MA (2018) MPCaD: a multi-scale radiomics-driven framework for automated prostate cancer localization and detection. BMC Med Imaging 18(1):16
29. Cuocolo R, Stanzione A, Ponsiglione A, Romeo V, Verde F, Creta M et al (2019) Clinically significant prostate cancer detection on MRI: a radiomic shape features study. Eur J Radiol 116:144–149
30. Merisaari H, Taimen P, Shiradkar R, Ettala O, Pesola M, Saunavaara J et al (2020) Repeatability of radiomics and machine learning for DWI: short-term repeatability study of 112 patients with prostate cancer. Magn Reson Med 83(6):2293–2309
31. Wong J, Fong A, McVicar N, Smith S, Giambattista J, Wells D et al (2020) Comparing deep learning-based auto-segmentation of organs at risk and clinical target volumes to expert inter-observer variability in radiotherapy planning. Radiother Oncol 144:152–158
32. Shiradkar R, Podder TK, Algohary A, Viswanath S, Ellis RJ, Madabhushi A (2016) Radiomics based targeted radiotherapy planning (Rad-TRaP): a computational framework for prostate cancer treatment planning with MRI. Radiat Oncol 11(1):148
33. Macomber MW, Phillips M, Tarapov I, Jena R, Nori A, Carter D et al (2018) Autosegmentation of prostate anatomy for radiation treatment planning using deep decision forests of radiomic features. Phys Med Biol 63(23):235002
34. Li M, Yang L, Yue Y, Xu J, Huang C, Song B (2020) Use of radiomics to improve diagnostic performance of PI-RADS v2.1 in prostate cancer. Front Oncol 10:631831
35. Harmon SA, Gesztes W, Young D, Mehralivand S, McKinney Y, Sanford T et al (2021) Prognostic features of biochemical recurrence of prostate cancer following radical prostatectomy based on multiparametric mrı and ımmunohistochemistry analysis of mrı-guided biopsy specimens. Radiology 2:202425
36. Wibmer AG, Robertson NL, Hricak H, Zheng J, Capanu M, Stone S et al (2019) Extracapsular extension on MRI indicates a more aggressive cell cycle progression genotype of prostate cancer. Abdom Radiol (NY) 44(8):2864–2873
37. Harmon SA, Gesztes W, Young D, Mehralivand S, McKinney Y, Sanford T et al (2021) Prognostic features of biochemical recurrence of prostate cancer following radical prostatectomy based on multiparametric mri and immunohistochemistry analysis of MRI-guided biopsy specimens. Radiology 299(3):613–623
38. Schelb P, Kohl S, Radtke JP, Wiesenfarth M, Kickingereder P, Bickelhaupt S et al (2019) Classification of cancer at prostate MRI: deep learning versus clinical PI-RADS assessment. Radiology 293(3):607–617
39. Vos PC, Barentsz JO, Karssemeijer N, Huisman HJ (2012) Automatic computer-aided detection of prostate cancer based on multiparametric magnetic resonance image analysis. Phys Med Biol 57(6):1527–1542
40. Winkel DJ, Wetterauer C, Matthias MO, Lou B, Shi B, Kamen A et al (2020) Autonomous detection and classification of PI-RADS lesions in an mrı screening population ıncorporating multicenter-labeled deep learning and biparametric ımaging: proof of concept. Diagnostics (Basel). 10:11
41. Muller BG, Shih JH, Sankineni S, Marko J, Rais-Bahrami S, George AK et al (2015) Prostate cancer: interobserver agreement and accuracy with the revised prostate imaging reporting and data system at multiparametric MR imaging. Radiology 277(3):741–750
42. Kobus T, Vos PC, Hambrock T, De Rooij M, Hulsbergen-Van de Kaa CA, Barentsz JO et al (2012) Prostate cancer aggressiveness: in vivo assessment of MR spectroscopy and diffusion-weighted imaging at 3T. Radiology 265(2):457–467
43. Peng Y, Jiang Y, Yang C, Brown JB, Antic T, Sethi I et al (2013) Quantitative analysis of multiparametric prostate MR images: differentiation between prostate cancer and normal tissue and correlation with Gleason score—a computer-aided diagnosis development study. Radiology 267(3):787–796
44. Nagarajan R, Margolis D, Raman S, Sarma MK, Sheng K, King CR et al (2012) MR spectroscopic imaging and diffusion-weighted imaging of prostate cancer with Gleason scores. J Magn Reson Imaging 36(3):697–703
45. Chan I, WellsMulkern WRV, Haker S, Zhang J, Zou KH et al (2003) Detection of prostate cancer by integration of line-scan diffusion, T2-mapping and T2-weighted magnetic resonance imaging; a multichannel statistical classifier. Med Phys 30(9):2390–2398
46. Langer DL, van der Kwast TH, Evans AJ, Trachtenberg J, Wilson BC, Haider MA (2009) Prostate cancer detection with multi-parametric MRI: logistic regression analysis of quantitative T2,

diffusion-weighted imaging, and dynamic contrast-enhanced MRI. J Magn Reson Imaging 30(2):327–334
47. Litjens G, Debats O, Barentsz J, Karssemeijer N, Huisman H (2014) Computer-aided detection of prostate cancer in MRI. IEEE Trans Med Imaging 33(5):1083–1092
48. Ferraro DA, Becker AS, Kranzbuhler B, Mebert I, Baltensperger A, Zeimpekis KG et al (2021) Diagnostic performance of (68) Ga-PSMA-11 PET/MRI-guided biopsy in patients with suspected prostate cancer: a prospective single-center study. Eur J Nucl Med Mol Imaging 2:2
49. Park SY, Zacharias C, Harrison C, Fan RE, Kunder C, Hatami N et al (2018) Gallium 68 PSMA-11 PET/MR imaging in patients with intermediate- or high-risk prostate cancer. Radiology 288(2):495–505
50. Hicks RM, Simko JP, Westphalen AC, Nguyen HG, Greene KL, Zhang L et al (2018) Diagnostic accuracy of (68)Ga-PSMA-11 PET/MRI compared with multiparametric mri in the detection of prostate cancer. Radiology 289(3):730–737
51. Pesapane F, Standaert C, De Visschere P, Villeirs G (2020) T-staging of prostate cancer: identification of useful signs to standardize detection of posterolateral extraprostatic extension on prostate MRI. Clin Imaging 59(1):1–7
52. Sala E, Akin O, Moskowitz CS, Eisenberg HF, Kuroiwa K, Ishill NM et al (2006) Endorectal MR imaging in the evaluation of seminal vesicle invasion: diagnostic accuracy and multivariate feature analysis. Radiology 238(3):929–937
53. de Rooij M, Hamoen EH, Witjes JA, Barentsz JO, Rovers MM (2016) Accuracy of magnetic resonance imaging for local staging of prostate cancer: a diagnostic meta-analysis. Eur Urol 70(2):233–245
54. Yu KK, Hricak H, Alagappan R, Chernoff DM, Bacchetti P, Zaloudek CJ (1997) Detection of extracapsular extension of prostate carcinoma with endorectal and phased-array coil MR imaging: multivariate feature analysis. Radiology 202(3):697–702
55. Wibmer A, Vargas HA, Donahue TF, Zheng J, Moskowitz C, Eastham J et al (2015) Diagnosis of extracapsular extension of prostate cancer on prostate MRI: impact of second-opinion readings by subspecialized genitourinary oncologic radiologists. AJR Am J Roentgenol 205(1):W73–W78
56. Cornejo KM, Rice-Stitt T, Wu CL (2020) Updates in staging and reporting of genitourinary malignancies. Arch Pathol Lab Med 144(3):305–319
57. Woo S, Kim SY, Cho JY, Kim SH (2017) Length of capsular contact on prostate MRI as a predictor of extracapsular extension: which is the most optimal sequence? Acta Radiol 58(4):489–497
58. Ukimura O, Troncoso P, Ramirez EI, Babaian RJ (1998) Prostate cancer staging: correlation between ultrasound determined tumor contact length and pathologically confirmed extraprostatic extension. J Urol 159(4):1251–1259
59. Woo S, Cho JY, Kim SY, Kim SH (2015) Extracapsular extension in prostate cancer: added value of diffusion-weighted MRI in patients with equivocal findings on T2-weighted imaging. AJR Am J Roentgenol 204(2):W168–W175
60. Wei CG, Zhang YY, Pan P, Chen T, Yu HC, Dai GC et al (2021) Diagnostic accuracy and interobserver agreement of PI-RADS version 2 and version 2.1 for the detection of transition zone prostate cancers. AJR Am J Roentgenol. 216(5):1247–1256
61. Woo S, Ghafoor S, Becker AS, Han S, Wibmer AG, Hricak H et al (2020) Prostate-specific membrane antigen positron emission tomography (PSMA-PET) for local staging of prostate cancer: a systematic review and meta-analysis. Eur J Hybrid Imaging 4(1):16
62. Draisma G, Boer R, Otto SJ, van der Cruijsen IW, Damhuis RA, Schroder FH et al (2003) Lead times and overdetection due to prostate-specific antigen screening: estimates from the European Randomized Study of Screening for Prostate Cancer. J Natl Cancer Inst 95(12):868–878
63. Carroll PR, Parsons JK, Andriole G, Bahnson RR, Castle EP, Catalona WJ et al (2016) NCCN guidelines insights: prostate cancer early detection, version 2.2016. J Natl Compr Canc Netw. 14(5):509–519
64. Sklinda K, Mruk B, Walecki J (2020) Active surveillance of prostate cancer using multiparametric magnetic resonance ımaging: a review of the current role and future perspectives. Med Sci Monit 26:e920252
65. Klotz L, Zhang L, Lam A, Nam R, Mamedov A, Loblaw A (2010) Clinical results of long-term follow-up of a large, active surveillance cohort with localized prostate cancer. J Clin Oncol 28(1):126–131
66. Shukla-Dave A, Hricak H, Akin O, Yu C, Zakian KL, Udo K et al (2012) Preoperative nomograms incorporating magnetic resonance imaging and spectroscopy for prediction of insignificant prostate cancer. BJU Int 109(9):1315–1322
67. Arabi A, Deebajah M, Yaguchi G, Pantelic M, Williamson S, Gupta N et al (2019) Systematic biopsy does not contribute to disease upgrading in patients undergoing targeted biopsy for PI-RADS 5 lesions identified on magnetic resonance imaging in the course of active surveillance for prostate cancer. Urology 134:168–172
68. Aus G, Abbou CC, Bolla M, Heidenreich A, Schmid HP, van Poppel H et al (2005) EAU guidelines on prostate cancer. Eur Urol 48(4):546–551
69. Del Monte M, Leonardo C, Salvo V, Grompone MD, Pecoraro M, Stanzione A et al (2018) MRI/US fusion-guided biopsy: performing exclusively targeted biopsies for the early detection of prostate cancer. Radiol Med 123(3):227–234
70. Bott SR, Young MP, Kellett MJ, Parkinson MC (2002) Contributors to the UCLHTRPD Anterior prostate cancer: is it more difficult to diagnose? BJU Int 89(9):886–889
71. Lawrentschuk N, Haider MA, Daljeet N, Evans A, Toi A, Finelli A et al (2010) "Prostatic evasive anterior tumours": the role of magnetic resonance imaging. BJU Int 105(9):1231–1236
72. Ploussard G, Beauval JB, Lesourd M, Almeras C, Assoun J, Aziza R et al (2020) Performance of systematic, MRI-targeted biopsies alone or in combination for the prediction of unfavourable disease in MRI-positive low-risk prostate cancer patients eligible for active surveillance. World J Urol 38(3):663–671
73. Sonn GA, Natarajan S, Margolis DJ, MacAiran M, Lieu P, Huang J et al (2013) Targeted biopsy in the detection of prostate cancer using an office based magnetic resonance ultrasound fusion device. J Urol 189(1):86–91
74. Ouzzane A, Puech P, Lemaitre L, Leroy X, Nevoux P, Betrouni N et al (2011) Combined multiparametric MRI and targeted biopsies improve anterior prostate cancer detection, staging, and grading. Urology 78(6):1356–1362
75. Ahmed HU, Hu Y, Carter T, Arumainayagam N, Lecornet E, Freeman A et al (2011) Characterizing clinically significant prostate cancer using template prostate mapping biopsy. J Urol 186(2):458–464
76. Siddiqui MM, Rais-Bahrami S, Turkbey B, George AK, Rothwax J, Shakir N et al (2015) Comparison of MR/ultrasound fusion-guided biopsy with ultrasound-guided biopsy for the diagnosis of prostate cancer. JAMA 313(4):390–397
77. Walton Diaz A, Shakir NA, George AK, Rais-Bahrami S, Turkbey B, Rothwax JT et al (2015) Use of serial multiparametric magnetic resonance imaging in the management of patients with prostate cancer on active surveillance. Urol Oncol 33(5):202
78. Rais-Bahrami S, Turkbey B, Rastinehad AR, Walton-Diaz A, Hoang AN, Siddiqui MM et al (2014) Natural history of small index lesions suspicious for prostate cancer on multiparametric

MRI: recommendations for interval imaging follow-up. Diagn Interv Radiol 20(4):293–298
79. Moore CM, Giganti F, Albertsen P, Allen C, Bangma C, Briganti A et al (2017) Reporting magnetic resonance imaging in men on active surveillance for prostate cancer: the PRECISE recommendations-a report of a european school of oncology task force. Eur Urol 71(4):648–655
80. Caglic I, Sushentsev N, Gnanapragasam VJ, Sala E, Shaida N, Koo BC et al (2021) MRI-derived PRECISE scores for predicting pathologically-confirmed radiological progression in prostate cancer patients on active surveillance. Eur Radiol 31(5):2696–2705
81. Kubler HR, Tseng TY, Sun L, Vieweg J, Harris MJ, Dahm P (2007) Impact of nerve sparing technique on patient self-assessed outcomes after radical perineal prostatectomy. J Urol 178(2):488–492
82. Preston MA, Breau RH, Lantz AG, Morash C, Gerridzen RG, Doucette S et al (2015) The association between nerve sparing and a positive surgical margin during radical prostatectomy. Urol Oncol 33(1):18
83. Nyarangi-Dix J, Wiesenfarth M, Bonekamp D, Hitthaler B, Schutz V, Dieffenbacher S et al (2020) Combined clinical parameters and multiparametric magnetic resonance imaging for the prediction of extraprostatic disease-a risk model for patient-tailored risk stratification when planning radical prostatectomy. Eur Urol Focus 6(6):1205–1212
84. Schiavina R, Bianchi L, Borghesi M, Dababneh H, Chessa F, Pultrone CV et al (2018) MRI displays the prostatic cancer anatomy and improves the bundles management before robot-assisted radical prostatectomy. J Endourol 32(4):315–321
85. Panebianco V, Salciccia S, Cattarino S, Minisola F, Gentilucci A, Alfarone A et al (2012) Use of multiparametric MR with neurovascular bundle evaluation to optimize the oncological and functional management of patients considered for nerve-sparing radical prostatectomy. J Sex Med 9(8):2157–2166
86. Couture F, Polesello S, Tholomier C, Bondarenko HD, Karakiewicz PI, Nazzani S et al (2019) Predictors of deviation in neurovascular bundle preservation during robotic prostatectomy. Can J Urol 26(1):9644–9653
87. Woo S, Han S, Kim TH, Suh CH, Westphalen AC, Hricak H et al (2020) Prognostic value of pretreatment MRI in patients with prostate cancer treated with radiation therapy: a systematic review and meta-analysis. AJR Am J Roentgenol 214(3):597–604
88. Kerkmeijer LGW, Groen VH, Pos FJ, Haustermans K, Monninkhof EM, Smeenk RJ et al (2021) Focal boost to the intraprostatic tumor in external beam radiotherapy for patients with localized prostate cancer: results from the FLAME randomized phase III trial. J Clin Oncol 39(7):787–796
89. Rosenkrantz AB, Scionti SM, Mendrinos S, Taneja SS (2011) Role of MRI in minimally invasive focal ablative therapy for prostate cancer. AJR Am J Roentgenol 197(1):W90–W96
90. Ramsay E, Mougenot C, Köhler M, Bronskill M, Klotz L, Haider MA et al (2013) MR thermometry in the human prostate gland at 3.0T for transurethral ultrasound therapy. J Magn Reson Imaging. 38(6):1564–1571
91. Shaikh F, Dupont-Roettger D, Dehmeshki J, Kubassova O, Quraishi MI (2020) Advanced imaging of biochemical recurrent prostate cancer with PET, MRI, and radiomics. Front Oncol 10:1359
92. Expert Panel on Urologic I, Froemming AT, Verma S, Eberhardt SC, Oto A, Alexander LF et al (2018) ACR Appropriateness criteria((R)) post-treatment follow-up prostate cancer. J Am Coll Radiol 15(5S):S132–S149
93. Barchetti F, Panebianco V (2014) Multiparametric MRI for recurrent prostate cancer post radical prostatectomy and postradiation therapy. Biomed Res Int 2014:316272
94. Rajwa P, Mori K, Huebner NA, Martin DT, Sprenkle PC, Weinreb JC et al (2021) The prognostic association of prostate MRI PI-RADS™ v2 assessment category and risk of biochemical recurrence after definitive local therapy for prostate cancer: a systematic review and meta-analysis. J Urol 206(3):507–516
95. Wibmer AG, Nikolovski I, Chaim J, Lakhman Y, Lefkowitz RA, Sala E et al (2021) Local extent of prostate cancer at mrı versus prostatectomy histopathology: associations with long-term oncologic outcomes. Radiology 2:210875
96. Woo S, Cho JY, Ku JH, Kim SY, Kim SH (2016) Prostate cancer-specific mortality after radical prostatectomy: value of preoperative MRI. Acta Radiol 57(8):1006–1013
97. Bhargava P, Ravizzini G, Chapin BF, Kundra V (2020) Imaging biochemical recurrence after prostatectomy: where are we headed? AJR Am J Roentgenol 214(6):1248–1258
98. Panebianco V, Villeirs G, Weinreb JC, Turkbey BI, Margolis DJ, Richenberg J et al (2021) Prostate magnetic resonance ımaging for local recurrence reporting (PI-RR): International consensus -based guidelines on multiparametric magnetic resonance ımaging for prostate cancer recurrence after radiation therapy and radical prostatectomy. Eur Urol Oncol 2:2
99. Vargas HA, Akin O, Hricak H (2010) Residual prostate tissue after radical prostatectomy: acceptable surgical complication or treatment failure? Urology 76(5):1136–1137
100. Sella T, Schwartz LH, Hricak H (2006) Retained seminal vesicles after radical prostatectomy: frequency, MRI characteristics, and clinical relevance. AJR Am J Roentgenol 186(2):539–546
101. Vargas HA, Martin-Malburet AG, Takeda T, Corradi RB, Eastham J, Wibmer A et al (2016) Localizing sites of disease in patients with rising serum prostate-specific antigen up to 1ng/ml following prostatectomy: How much information can conventional imaging provide? Urol Oncol 34(11):482
102. Vargas HA, Wassberg C, Akin O, Hricak H (2012) MR imaging of treated prostate cancer. Radiology 262(1):26–42
103. Wu LM, Xu JR, Gu HY, Hua J, Zhu J, Chen J et al (2013) Role of magnetic resonance imaging in the detection of local prostate cancer recurrence after external beam radiotherapy and radical prostatectomy. Clin Oncol (R Coll Radiol) 25(4):252–264
104. Roy C, Foudi F, Charton J, Jung M, Lang H, Saussine C et al (2013) Comparative sensitivities of functional MRI sequences in detection of local recurrence of prostate carcinoma after radical prostatectomy or external-beam radiotherapy. AJR Am J Roentgenol 200(4):W361–W368
105. Sciarra A, Panebianco V, Salciccia S, Osimani M, Lisi D, Ciccariello M et al (2008) Role of dynamic contrast-enhanced magnetic resonance (MR) imaging and proton MR spectroscopic imaging in the detection of local recurrence after radical prostatectomy for prostate cancer. Eur Urol 54(3):589–600
106. Panebianco V, Barchetti F, Sciarra A, Musio D, Forte V, Gentile V et al (2013) Prostate cancer recurrence after radical prostatectomy: the role of 3-T diffusion imaging in multi-parametric magnetic resonance imaging. Eur Radiol 23(6):1745–1752
107. Cha D, Kim CK, Park SY, Park JJ, Park BK (2015) Evaluation of suspected soft tissue lesion in the prostate bed after radical prostatectomy using 3T multiparametric magnetic resonance imaging. Magn Reson Imaging 33(4):407–412
108. Coppola A, Platania G, Ticca C, De Mattia C, Bortolato B, Palazzi MF et al (2020) Sensitivity of CE-MRI in detecting local recurrence after radical prostatectomy. Radiol Med 125(7):683–690
109. Kitajima K, Hartman RP, Froemming AT, Hagen CE, Takahashi N, Kawashima A (2015) Detection of local recurrence of prostate cancer after radical prostatectomy using endorectal coil MRI at 3 T: addition of DWI and dynamic contrast enhancement to T2-weighted MRI. AJR Am J Roentgenol 205(4):807–816

110. Mazaheri Y, Akin O, Hricak H (2017) Dynamic contrast-enhanced magnetic resonance imaging of prostate cancer: a review of current methods and applications. World J Radiol 9(12):416–425
111. Boonsirikamchai P, Kaur H, Kuban DA, Jackson E, Hou P, Choi H (2012) Use of maximum slope images generated from dynamic contrast-enhanced MRI to detect locally recurrent prostate carcinoma after prostatectomy: a practical approach. AJR Am J Roentgenol 198(3):W228–W236
112. Parra NA, Orman A, Padgett K, Casillas V, Punnen S, Abramowitz M et al (2017) Dynamic contrast-enhanced MRI for automatic detection of foci of residual or recurrent disease after prostatectomy. Strahlenther Onkol 193(1):13–21
113. Donati OF, Jung SI, Vargas HA, Gultekin DH, Zheng J, Moskowitz CS et al (2013) Multiparametric prostate MR imaging with T2-weighted, diffusion-weighted, and dynamic contrast-enhanced sequences: are all pulse sequences necessary to detect locally recurrent prostate cancer after radiation therapy? Radiology 268(2):440–450
114. Song I, Kim CK, Park BK, Park W (2010) Assessment of response to radiotherapy for prostate cancer: value of diffusion-weighted MRI at 3 T. AJR Am J Roentgenol 194(6):W477–W482
115. Wu X, Reinikainen P, Kapanen M, Vierikko T, Ryymin P, Kellokumpu-Lehtinen PL (2017) Diffusion-weighted MRI provides a useful biomarker for evaluation of radiotherapy efficacy in patients with prostate cancer. Anticancer Res 37(9):5027–5032
116. Pasquier D, Hadj Henni A, Escande A, Tresch E, Reynaert N, Colot O et al (2018) Diffusion weighted MRI as an early predictor of tumor response to hypofractionated stereotactic boost for prostate cancer. Sci Rep 8(1):10407
117. Morgan VA, Riches SF, Giles S, Dearnaley D, deSouza NM (2012) Diffusion-weighted MRI for locally recurrent prostate cancer after external beam radiotherapy. AJR Am J Roentgenol 198(3):596–602
118. Lee SL, Lee J, Craig T, Berlin A, Chung P, Menard C et al (2019) Changes in apparent diffusion coefficient radiomics features during dose-painted radiotherapy and high dose rate brachytherapy for prostate cancer. Phys Imaging Radiat Oncol 9:1–6
119. van der Poel HG, van den Bergh RCN, Briers E, Cornford P, Govorov A, Henry AM et al (2018) Focal therapy in primary localised prostate cancer: the European Association of urology position in 2018. Eur Urol 74(1):84–91
120. Kirkham AP, Emberton M, Hoh IM, Illing RO, Freeman AA, Allen C (2008) MR imaging of prostate after treatment with high-intensity focused ultrasound. Radiology 246(3):833–844
121. Ghafoor S, Becker AS, Stocker D, Barth BK, Eberli D, Donati OF et al (2020) Magnetic resonance imaging of the prostate after focal therapy with high-intensity focused ultrasound. Abdom Radiol (NY) 45(11):3882–3895
122. Lotte R, Lafourcade A, Mozer P, Conort P, Barret E, Comperat E et al (2018) Multiparametric MRI for suspected recurrent prostate cancer after HIFU: Is DCE still needed? Eur Radiol 28(9):3760–3769
123. McKay RR, Feng FY, Wang AY, Wallis CJD, Moses KA (2020) Recent advances in the management of high-risk localized prostate cancer: local therapy, systemic therapy, and biomarkers to guide treatment decisions. Am Soc Clin Oncol Educ Book 40:1–12
124. Kim AY, Kim CK, Park SY, Park BK (2014) Diffusion-weighted imaging to evaluate for changes from androgen deprivation therapy in prostate cancer. AJR Am J Roentgenol 203(6):W645–W650
125. Daniel M, Kuess P, Andrzejewski P, Nyholm T, Helbich T, Polanec S et al (2019) Impact of androgen deprivation therapy on apparent diffusion coefficient and T2w MRI for histogram and texture analysis with respect to focal radiotherapy of prostate cancer. Strahlenther Onkol 195(5):402–411
126. Hotker AM, Mazaheri Y, Zheng J, Moskowitz CS, Berkowitz J, Lantos JE et al (2015) Prostate cancer: assessing the effects of androgen-deprivation therapy using quantitative diffusion-weighted and dynamic contrast-enhanced MRI. Eur Radiol 25(9):2665–2672
127. Padhani AR, MacVicar AD, Gapinski CJ, Dearnaley DP, Parker GJ, Suckling J et al (2001) Effects of androgen deprivation on prostatic morphology and vascular permeability evaluated with mr imaging. Radiology 218(2):365–374
128. Alonzi R, Padhani AR, Taylor NJ, Collins DJ, D'Arcy JA, Stirling JJ et al (2011) Antivascular effects of neoadjuvant androgen deprivation for prostate cancer: an in vivo human study using susceptibility and relaxivity dynamic MRI. Int J Radiat Oncol Biol Phys 80(3):721–727
129. Bjoreland U, Nyholm T, Jonsson J, Skorpil M, Blomqvist L, Strandberg S et al (2021) Impact of neoadjuvant androgen deprivation therapy on magnetic resonance imaging features in prostate cancer before radiotherapy. Phys Imaging Radiat Oncol 17:117–123
130. Mota JM, Armstrong AJ, Larson SM, Fox JJ, Morris MJ (2019) Measuring the unmeasurable: automated bone scan index as a quantitative endpoint in prostate cancer clinical trials. Prostate Cancer Prostatic Dis 22(4):522–530
131. Woo S, Suh CH, Kim SY, Cho JY, Kim SH (2018) Diagnostic performance of magnetic resonance imaging for the detection of bone metastasis in prostate cancer: a systematic review and meta-analysis. Eur Urol 73(1):81–91
132. Summers P, Saia G, Colombo A, Pricolo P, Zugni F, Alessi S et al (2021) Whole-body magnetic resonance imaging: technique, guidelines and key applications. Ecancermedicalscience 15:1164
133. Turpin A, Girard E, Baillet C, Pasquier D, Olivier J, Villers A et al (2020) Imaging for metastasis in prostate cancer: a review of the literature. Front Oncol 10:55
134. Hofman MS, Lawrentschuk N, Francis RJ, Tang C, Vela I, Thomas P et al (2020) Prostate-specific membrane antigen PET-CT in patients with high-risk prostate cancer before curative-intent surgery or radiotherapy (proPSMA): a prospective, randomised, multicentre study. Lancet 395(10231):1208–1216
135. Calais J, Ceci F, Eiber M, Hope TA, Hofman MS, Rischpler C et al (2019) (18)F-fluciclovine PET-CT and (68)Ga-PSMA-11 PET-CT in patients with early biochemical recurrence after prostatectomy: a prospective, single-centre, single-arm, comparative imaging trial. Lancet Oncol 20(9):1286–1294
136. Perez-Lopez R, Tunariu N, Padhani AR, Oyen WJG, Fanti S, Vargas HA et al (2019) Imaging diagnosis and follow-up of advanced prostate cancer: clinical perspectives and state of the art. Radiology 292(2):273–286
137. Barchetti F, Stagnitti A, Megna V, Al Ansari N, Marini A, Musio D et al (2016) Unenhanced whole-body MRI versus PET-CT for the detection of prostate cancer metastases after primary treatment. Eur Rev Med Pharmacol Sci 20(18):3770–3776
138. Woo S, Kim SY, Kim SH, Cho JY (2016) JOURNAL CLUB: identification of bone metastasis with routine prostate MRI: A study of patients with newly diagnosed prostate cancer. AJR Am J Roentgenol 206(6):1156–1163
139. Jambor I, Kuisma A, Ramadan S, Huovinen R, Sandell M, Kajander S et al (2016) Prospective evaluation of planar bone scintigraphy, SPECT, SPECT/CT, 18F-NaF PET/CT and whole body 1.5T MRI, including DWI, for the detection of bone metastases in high risk breast and prostate cancer patients: SKELETA clinical trial. Acta Oncol 55(1):59–67
140. Johnston EW, Latifoltojar A, Sidhu HS, Ramachandran N, Sokolska M, Bainbridge A et al (2019) Multiparametric whole-body 3.0-T MRI in newly diagnosed intermediate- and high-risk

prostate cancer: diagnostic accuracy and interobserver agreement for nodal and metastatic staging. Eur Radiol. 29(6):3159–3169
141. Shen G, Deng H, Hu S, Jia Z (2014) Comparison of choline-PET/CT, MRI, SPECT, and bone scintigraphy in the diagnosis of bone metastases in patients with prostate cancer: a meta-analysis. Skeletal Radiol 43(11):1503–1513
142. Perez-Lopez R, Lorente D, Blackledge MD, Collins DJ, Mateo J, Bianchini D et al (2016) Volume of bone metastasis assessed with whole-body diffusion-weighted imaging is associated with overall survival in metastatic castration-resistant prostate cancer. Radiology 280(1):151–160
143. Reischauer C, Froehlich JM, Koh DM, Graf N, Padevit C, John H et al (2010) Bone metastases from prostate cancer: assessing treatment response by using diffusion-weighted imaging and functional diffusion maps–initial observations. Radiology 257(2):523–531
144. Reischauer C, Patzwahl R, Koh DM, Froehlich JM, Gutzeit A (2018) Texture analysis of apparent diffusion coefficient maps for treatment response assessment in prostate cancer bone metastases-A pilot study. Eur J Radiol 101:184–190
145. Lebastchi AH, Gupta N, DiBianco JM, Piert M, Davenport MS, Ahdoot MA et al (2020) Comparison of cross-sectional imaging techniques for the detection of prostate cancer lymph node metastasis: a critical review. Transl Androl Urol 9(3):1415–1427
146. Woo S, Suh CH, Kim SY, Cho JY, Kim SH (2018) The diagnostic performance of MRI for detection of lymph node metastasis in bladder and prostate cancer: an updated systematic review and diagnostic meta-analysis. AJR Am J Roentgenol 210(3):W95–W109
147. Hovels AM, Heesakkers RA, Adang EM, Jager GJ, Strum S, Hoogeveen YL et al (2008) The diagnostic accuracy of CT and MRI in the staging of pelvic lymph nodes in patients with prostate cancer: a meta-analysis. Clin Radiol 63(4):387–395
148. Vallini V, Ortori S, Boraschi P, Manassero F, Gabelloni M, Faggioni L et al (2016) Staging of pelvic lymph nodes in patients with prostate cancer: usefulness of multiple b value SE-EPI diffusion-weighted imaging on a 3.0 T MR system. Eur J Radiol Open. 3:16–21
149. Eiber M, Beer AJ, Holzapfel K, Tauber R, Ganter C, Weirich G et al (2010) Preliminary results for characterization of pelvic lymph nodes in patients with prostate cancer by diffusion-weighted MR-imaging. Invest Radiol 45(1):15–23
150. Thoeny HC, Froehlich JM, Triantafyllou M, Huesler J, Bains LJ, Vermathen P et al (2014) Metastases in normal-sized pelvic lymph nodes: detection with diffusion-weighted MR imaging. Radiology 273(1):125–135
151. Heesakkers RA, Hövels AM, Jager GJ, van den Bosch HC, Witjes JA, Raat HP et al (2008) MRI with a lymph-node-specific contrast agent as an alternative to CT scan and lymph-node dissection in patients with prostate cancer: a prospective multicohort study. Lancet Oncol 9(9):850–856
152. Schilham MG, Zamecnik P, Prive BM, Israel B, Rijpkema M, Scheenen T et al (2021) Head-to-head comparison of (68)Ga-prostate-specific membrane antigen PET/CT and ferumoxtran-10 enhanced MRI for the diagnosis of lymph node metastases in prostate cancer patients. J Nucl Med 2:2
153. Birkhäuser FD, Studer UE, Froehlich JM, Triantafyllou M, Bains LJ, Petralia G et al (2013) Combined ultrasmall superparamagnetic particles of iron oxide-enhanced and diffusion-weighted magnetic resonance imaging facilitates detection of metastases in normal-sized pelvic lymph nodes of patients with bladder and prostate cancer. Eur Urol 64(6):953–960
154. Padhani AR, Lecouvet FE, Tunariu N, Koh DM, De Keyzer F, Collins DJ et al (2017) Metastasis reporting and data system for prostate cancer: practical guidelines for acquisition, interpretation, and reporting of whole-body magnetic resonance imaging-based evaluations of multiorgan involvement in advanced prostate cancer. Eur Urol 71(1):81–92
155. Evangelista L, Zattoni F, Cassarino G, Artioli P, Cecchin D, Dal Moro F et al (2021) PET/MRI in prostate cancer: a systematic review and meta-analysis. Eur J Nucl Med Mol Imaging 48(3):859–873
156. Galgano SJ, McDonald AM, Rais-Bahrami S, Porter KK, Choudhary G, Burgan C et al (2020) Utility of (18)F-fluciclovine PET/MRI for staging newly diagnosed high-risk prostate cancer and evaluating response to ınitial androgen deprivation therapy: a prospective single-arm pilot study. AJR Am J Roentgenol 2:2
157. Souvatzoglou M, Eiber M, Takei T, Furst S, Maurer T, Gaertner F et al (2013) Comparison of integrated whole-body [11C]choline PET/MR with PET/CT in patients with prostate cancer. Eur J Nucl Med Mol Imaging 40(10):1486–1499